

# Demystifying Video Reasoning

Ruisi Wang<sup>1</sup>, Zhongang Cai<sup>✉,1</sup>, Fanyi Pu<sup>1,2</sup>, Junxiang Xu<sup>1</sup>, Wanqi Yin<sup>1</sup>,  
Maijunixian Wang<sup>3</sup>, Ran Ji<sup>4</sup>, Chenyang Gu<sup>1</sup>, Bo Li<sup>2</sup>, Ziqi Huang<sup>2</sup>,  
Hokin Deng<sup>5</sup>, Dahua Lin<sup>1</sup>, Ziwei Liu<sup>2</sup>, Lei Yang<sup>1</sup>

✉ Corresponding Author

<sup>1</sup> SenseTime Research   <sup>2</sup> Nanyang Technological University   <sup>3</sup> University of California, Berkeley

<sup>4</sup> University of California, San Diego   <sup>5</sup> Carnegie Mellon University

## Abstract

Recent advances in video generation have revealed an unexpected phenomenon: diffusion-based video models exhibit non-trivial reasoning capabilities. Prior work attributes this to a Chain-of-Frames (CoF) mechanism, where reasoning is assumed to unfold sequentially across video frames. In this work, we challenge this assumption and uncover a fundamentally different mechanism. We show that reasoning in video models instead primarily emerges along the *diffusion denoising steps*. Through qualitative analysis and targeted probing experiments, we find that models explore multiple candidate solutions in early denoising steps and progressively converge to a final answer, a process we term **Chain-of-Steps (CoS)**. Beyond this core mechanism, we identify several emergent reasoning behaviors critical to model performance: (1) **working memory**, enabling persistent reference; (2) **self-correction and enhancement**, allowing recovery from incorrect intermediate solutions; and (3) **perception before action**, where early steps establish semantic grounding and later steps perform structured manipulation. During a diffusion step, we further uncover self-evolved **functional specialization** within Diffusion Transformers, where early layers encode dense perceptual structure, middle layers execute reasoning, and later layers consolidate latent representations. Motivated by these insights, we present a simple training-free strategy as a proof-of-concept, demonstrating how reasoning can be improved by ensembling latent trajectories from identical models with different random seeds. Overall, our work provides a systematic understanding of how reasoning emerges in video generation models, offering a foundation to guide future research in better exploiting the inherent reasoning dynamics of video models as a new substrate for intelligence.

Homepage: [https://www.wrui.com/demystifying\\_video\\_reasoning](https://www.wrui.com/demystifying_video_reasoning)

## 1 Introduction

Video generation models have transformed the landscape of movie, gaming, and entertainment industries. However, most research has focused primarily on their ability to produce high-fidelity, realistic, and visually appealing videos. Recent advances have revealed an unexpected phenomenon: diffusion-based video models exhibit non-trivial reasoning capabilities in spatiotemporally consistent visual environments [62]. Prior work attributes this behavior to a Chain-of-Frames (CoF) mechanism, suggesting that reasoning unfolds sequentially across video frames. Despite this intriguing discovery, the underlying mechanisms of video reasoning remain largely unexplored. With the recent release of large-scale video reasoning datasets and open-source foundation models [58], we now have the opportunity to systematically investigate this capability. Leveraging these resources, we conduct the first comprehensive dissection of video reasoning and uncover a fundamentally different mechanism: reasoning in diffusion-based video models primarily emerges along the denoising process rather than across frames.

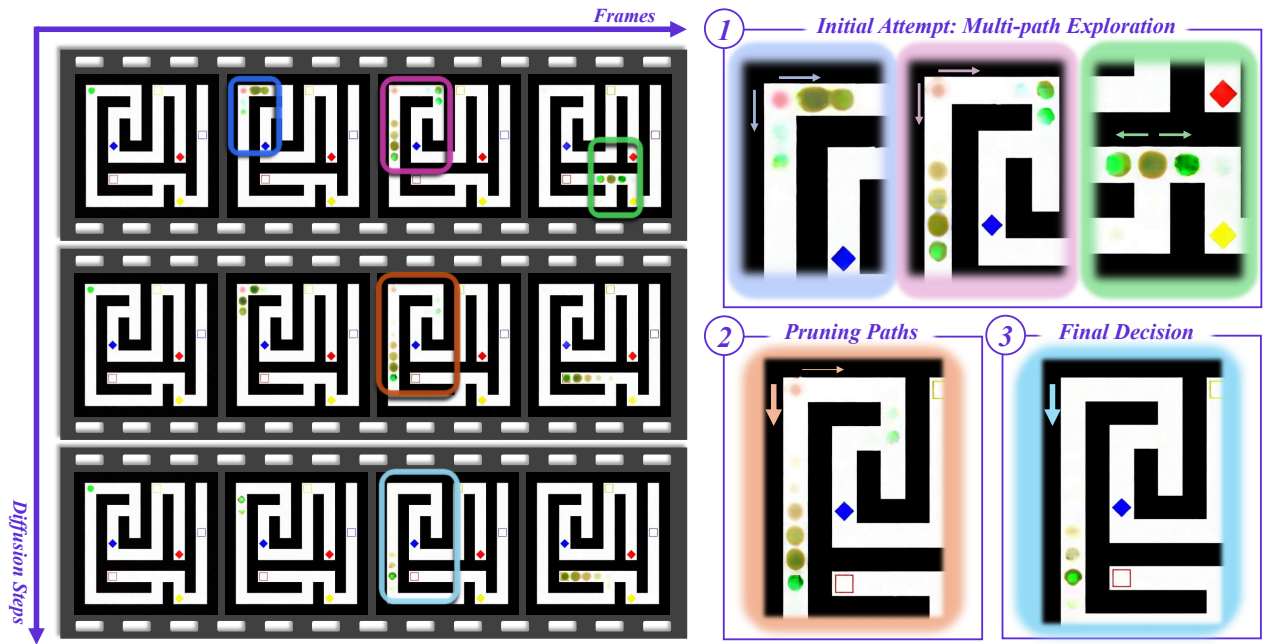


**Figure 1 Chain-of-Steps.** We discover that video reasoning occurs along the diffusion steps with surprising emergent behaviors such as making multiple possible moves (*e.g.*, paths) simultaneously at early steps, gradually pruning suboptimal choices during middle steps, and reaching a final decision at the late steps. This maze-solving example asks the model to start from the green circle in the top-left corner and find the red rectangle. Key regions of interest are color-coded and enlarged on the right.

Our key discovery challenges the prevailing Chain-of-Frames (CoF) hypothesis [62, 66], which assumes that video reasoning unfolds sequentially across frames. Instead, we find that reasoning does not primarily operate along the temporal dimension. Rather, it emerges along the diffusion denoising steps, progressing throughout generation. We term this mechanism **Chain-of-Steps (CoS)**. This finding suggests a fundamentally different view of how diffusion-based video models reason. Due to bidirectional attention over the entire sequence, reasoning is performed across all frames simultaneously at each denoising step, with intermediate hypotheses progressively refined as the process unfolds. Qualitative analysis reveals intriguing dynamics. In early denoising steps, the model often entertains multiple possibilities (populating alternative trajectories or superimposing candidate outcomes) before gradually converging to a final solution in later steps. Moreover, noise perturbation analysis shows that disruptions at specific denoising steps significantly degrade performance, whereas frame-wise perturbations have a much weaker impact. Further information propagation analysis identifies that the conclusion primarily solidifies during the middle diffusion steps.

Furthermore, we uncover several surprising emergent behaviors in video reasoning models that are strikingly similar to those observed in early studies of Large Language Models (LLMs). First, these models exhibit a form of **working memory** that is crucial for tasks requiring persistent references (*e.g.*, object permanence). Second, we observe that video models can **self-correct** errors during the CoS reasoning process, rather than committing to incorrect trajectories throughout generation. Third, video models exhibit a **"perception before action"** behavior, where early diffusion steps prioritize localizing target objects before subsequent steps perform more complex reasoning and manipulation.

We further conduct a fine-grained analysis of the Diffusion Transformer by examining token representations within a single diffusion step. This reveals the self-evolved, diverse, task-agnostic functional layers throughout the network. Within a diffusion step, early layers focus on dense perceptual understanding (*e.g.*, separating foreground from background and identifying basic geometric structures), while a set of critical middle layers performs the bulk of the reasoning. The final layers then consolidate the latent representation to produce the video state for the next step.

Motivated by these insights, we present a simple *training-free* method as a proof-of-concept for improving video reasoning models. Given that the model inherently explores multiple reasoning paths during the diffusion process, we propose an inference-time ensemble strategy that merges latents produced by three identical models with different random seeds. This approach encourages the model to retain a richer set of candidate reasoning trajectories during generation. As a result, the model explores more diverse reasoning paths and is more likely to converge to the correct solution, illustrating a way to utilize our findings to design more effective video reasoning systems.

In summary, we investigate the underlying mechanisms of video reasoning in diffusion models and identify Chain-of-Steps (CoS), a reasoning process that unfolds along the denoising trajectory. We further uncover several emergent reasoning behaviors that arise in these models. Building on these insights, we demonstrate how such mechanisms can be exploited through a simple training-free strategy for reasoning path ensembling. We believe our findings provide a foundation for understanding and advancing video reasoning, positioning it as a promising next-generation substrate for machine intelligence.

## 2 Related Works

### 2.1 Reasoning in Language and Multimodal Models

Recent studies show that large language models (LLMs) exhibit remarkable reasoning capabilities. Early work identifies emergent behaviors that arise as models scale in size and data [60], and demonstrates that Chain-of-Thought (CoT) prompting, which elicits intermediate reasoning steps, significantly improves performance [61]. Subsequent work explores mechanisms such as self-reflection, correction, and action [21, 39, 69, 72]. Coconut further suggests that reasoning can also occur implicitly within latent representations [18]. Meanwhile, research has increasingly explored extending reasoning beyond language into multimodal settings. Early progress in vision-language models (VLMs) enables reasoning over images in addition to text [1, 2, 6, 32, 37], whereas recent work has studied unified architectures that jointly model language and vision [4, 8, 14, 33, 42, 46, 54, 56, 64, 65, 80, 81]. These architectures empower reasoning for generation [10, 16, 27, 34, 50, 67, 79], enable reasoning with generation through visual CoT [5, 7, 13, 23, 25, 31, 45, 51, 68], and extend to embodied scenarios [74–76]. Together, these findings suggest that reasoning over multimodal signals opens up avenues for advanced reasoning capabilities. However, these efforts remain limited to discrete text and static images, making it challenging to leverage spatiotemporally consistent priors. Our work aims to investigate video as the next substrate for reasoning in intelligent systems.

### 2.2 Video Generation Models

Video generation has advanced rapidly with the development of diffusion models [20, 47] and high-fidelity variational autoencoders (VAEs) [9, 26, 77]. While early approaches focus primarily on generating short clips, the emergence of Diffusion Transformers (DiTs) [43] has enabled effective scaling of data and model size. As a result, recent video generators [11, 15, 28, 30, 41, 48, 57, 59] achieve impressive visual fidelity. Despite these advances, major challenges remain in physical plausibility [73, 78], commonsense knowledge [78], and spatiotemporal reasoning [38, 58, 62]. Consequently, recent research has begun shifting toward investigating the reasoning capabilities of video generation models. One line of work leverages the reasoning abilities of multimodal LLMs to guide video synthesis. For example, VChain [23] and MetaCanvas [35] incorporate external reasoning modules into pre-trained generators, while Omni-Video [53] uses symbolic reasoning from LLMs to guide generation. More recently, several studies ask whether video generators themselves can perform reasoning without external supervision, treating them as zero-shot learners operating in a spatiotemporal environments [19, 55, 62]. However, the mechanisms underlying this capability remain unexplored. Our work addresses this gap by investigating the internal reasoning processes of diffusion-based video models.

### 2.3 Similarities to Biological Brains

The diffusion model may be doing something analogous to how biological brains plan and think. For example, when a rat is deciding which path to take to reach food, researchers have observed that multiple simulated trajectories are rolled out in the hippocampus during the planning phase. In these experiments, the rat is held still first, and only after a delay period is it allowed to move [44]. Recent work suggests that human brains may employ analogous mechanisms for planning and internal simulation during conceptual reasoning and decision-making [3, 40].

## 3 Chain-of-Steps: Reasoning along Diffusion Steps

While prior work [62] hypothesizes a *Chain-of-Frames* (CoF) mechanism in which reasoning in video models unfolds frame by frame, generated frames appear to exhibit a “causal” property where later frames gradually build conclusions conditioned on earlier frames. However, our analysis of the underlying video reasoning mechanism reveals evidence to the contrary. First, we empirically analyze a wide range of reasoning tasks and find that the core logical reasoning in video generation models occurs across the diffusion denoising steps (Sec. 3.1). Diffusion steps do more than merely

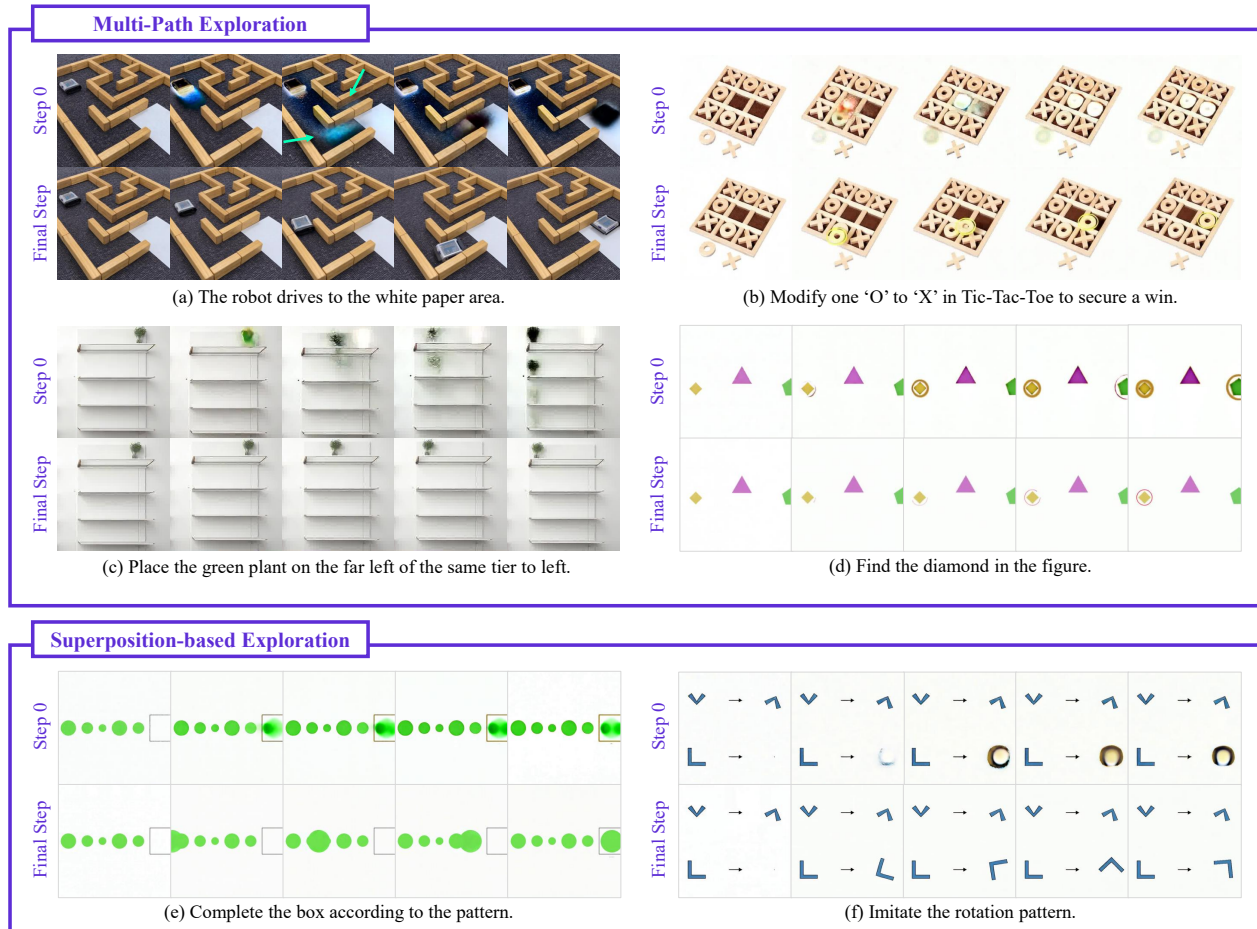


**Figure 2 Chain-of-Steps elicits reasoning along the diffusion process.** We observe that video reasoning models explore multiple possible solutions simultaneously in the early denoising steps before converging to a final outcome in later steps. Specifically, we observe: (a) two potential routes (cyan arrows highlight the "imaginary traces") for the robot; (b) two possible placements of the "O" piece; (c) multiple candidate end positions for the plant; (d) simultaneous selection of two diamonds; (e) large and small circles overlapping with each other; and (f) all possible rotations of the L-shaped object superimposed.

refine visual texture; instead, they explore multiple possibilities, evaluate their plausibility, and gradually converge to the correct outcome through the denoising process. Second, we introduce noise perturbations to disrupt information flow at both the frame and step levels (Sec. 3.2). Our findings reaffirm that CoS, rather than CoF, more accurately characterizes the reasoning mechanism in video models.

### 3.1 Diffusion Steps as the Primary Axis of Reasoning

If not otherwise stated, we base our study on VBVR-Wan2.2 [58], the latest video reasoning model finetuned from the powerful Wan2.2-I2V-A14B [57] on unprecedentedly large-scale video reasoning data. We extract test cases mainly from video reasoning benchmarks such as VBVR [58] and general video generation benchmarks such as VBench [22, 24].

To observe the model’s internal decision-making dynamics, we examine the estimated clean latent  $\hat{x}_0$  at each diffusion step  $s$ . Diffusion-based generative models progressively transform noise into structured data through an iterative denoising process. When trained with flow matching[36], the latent evolves along a continuous transport path between noise and data:

$$x_s = (1 - s)x_0 + sx_1 \quad (1)$$

where  $x_0$  is the clean latent and  $x_1 \sim \mathcal{N}(\mathbf{0}, \mathbf{I})$  is noise. The model learns a velocity field  $v_\theta(x_s, s, c)$  conditioned on prompt  $c$ , describing how the latent moves along this trajectory. The noise scale  $\sigma_s$  controls the magnitude of perturbation

at each step. Therefore, the intermediate decoded state is estimated by removing the predicted noise component:

$$\hat{x}_0 = x_s - \sigma_s \cdot v_\theta(x_s, s, c) \quad (2)$$

By decoding  $\hat{x}_0$  at each diffusion step, we can visualize how semantic decisions evolve and analyze the model’s intermediate reasoning dynamics.

Analogous to LLMs that exhibits reasoning behaviors along chain-of-thought, where the model gradually reaches its conclusion, to our surprise, we discover a similar scheme in video reasoning models along diffusion denoising steps. Specifically, we consistently observe a shared behavioral pattern that early diffusion steps act as a high-level heuristic search. During this stage, the model populates the latent workspace with multiple hypotheses. As denoising progresses, the model effectively "prunes" the solution tree, converging toward a logically consistent output.

This is exemplified in Fig. 1, for complex navigational tasks such as maze-solving, the decoded latent prediction  $\hat{x}_0$  after early diffusion steps appear as a probabilistic cloud in which several plausible paths are spawned and explored in parallel. Over subsequent steps, suboptimal trajectories gradually get suppressed, converging towards the final solution. By analyzing intermediate latent predictions at each step, we move beyond the "Chain-of-Frames" (CoF) temporal analogy and identify two distinct modes of Step-wise Reasoning: Multi-path Exploration and Superposition-based Exploration.

### 3.1.1 Multi-Path Exploration.

In high-complexity logical tasks, the diffusion process resembles a Breadth-First Search (BFS) or a multi-choice elimination procedure, where the model explores a tree of possible solutions and gradually prunes incorrect branches. It is worth noting that this behavior is reminiscent of the parallel reasoning trajectories explicitly studied in the LLM community (e.g., Tree of Thoughts [71]). However, video generation models naturally explore multiple solution paths in parallel during the diffusion process, inherently performing a similar form of structured search within their latent space. In some tasks involving object movements, the model explicitly visualizes this exploration process through multiple motion trajectories. In other tasks where the model must select an action from a discrete set of alternatives, we observe that the model initially considers several actions simultaneously and progressively discards candidates as the denoising process proceeds, until only a single valid outcome remains.

- *Fig. 2(a) Robot Navigation.* The intermediate steps show the robot simultaneously exploring both the upper and lower routes through the maze. As the diffusion process proceeds, the trajectory corresponding to the lower path becomes increasingly dominant, while the alternative route gradually disappears, indicating that the model chooses the final path.
- *Fig. 2(b) Tic-Tac-Toe.* During the early reasoning stage, the model simultaneously highlights multiple candidate cells that for a winning move.
- *Fig. 2(c) Object Movement.* In this example, it is clearly observable that at the early stage, the model proposes four potential trajectories corresponding to the four layers on the left side of the shelf. As the denoising steps continue, these alternatives gradually collapse toward placing the plant on the first layer, producing a clear and consistent motion path.
- *Fig. 2(d) Diamond Detection.* The model initially marks two candidate shapes that might satisfy the query. Through iterative refinement, the incorrect candidate fades; only the correct diamond remain circled in the end.

### 3.1.2 Superposition-based Exploration

Another distinctive mode observable along the diffusion trajectory is superposition-based exploration, where the model temporarily represents multiple mutually exclusive logical states simultaneously. Instead of committing early to a single configuration, the model maintains overlapping hypotheses that gradually resolve as noise is removed. This phenomenon is particularly evident in tasks involving object reordering and spatial alignment.

- *Fig. 2(e) Size Pattern Completion.* The size-pattern follows a repeating "large-medium–small" pattern. When predicting the next element, the model initially generates overlapping circles of different sizes, representing competing hypotheses about the correct continuation of the sequence.

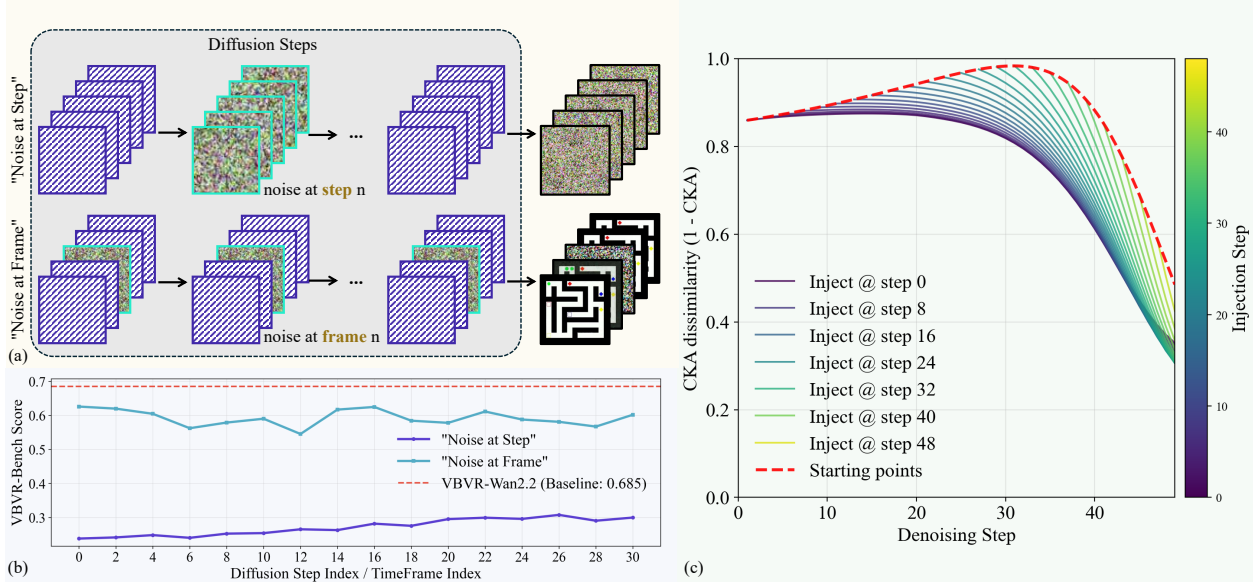


**Figure 3 Noise perturbation and information flow.** (a) Illustration of noise injection schemes; "Noise at Step" suffers more significant corruption than "Noise at Frame". (b) Performance drop with the two noise injection schemes. X-axis is the injection index (either diffusion step or frame). (c) Information flow across denoising steps (CKA dissimilarity: 1.0 indicates complete corruption, 0.0 indicates no effect).

- *Fig. 2(f) Objects Rotation.* In this task, rather than rotating discretely from one angle to another, the model produces a blurred representation of several candidate orientations.

### 3.2 Noise Perturbation and Information Flow

Our hypothesis is further validated through targeted noise injection experiments. We compare two settings to isolate where the core reasoning process occurs: 1) "Noise at Step":  $x_{s,\forall f} \leftarrow \mathcal{N}(0, \mathbf{I})$ . That is, disruptive Gaussian noise is injected into all frames at a specific diffusion step. 2) "Noise at Frame":  $x_{\forall s,f} \leftarrow \mathcal{N}(0, \mathbf{I})$ . That is, Gaussian noise is injected into a specific frame across all diffusion steps. The two settings are illustrated in Fig. 3(a).

In Fig. 3(b), we evaluate model performance under these two noise injection schemes. Compared to the baseline without noise, the "Noise at Step" setting causes the final score to collapse from 0.685 to below 0.3, indicating that the reasoning trajectory is highly sensitive to disruptions along the diffusion steps. Noise injected at a particular diffusion step therefore leads to a significant interruption of the model's reasoning process.

In contrast, under "Noise at Frame" injection, the model demonstrates more robustness with a much smaller performance drop. This behavior can be explained by the architecture of diffusion transformers: each denoising step has full observation of the preceding latent sequence through bidirectional attention, allowing the model to refine the entire video latent jointly. Consequently, corrupted frames can be recovered by leveraging the uncorrupted information from neighboring frames during subsequent denoising steps.

In Fig. 3(c), we further analyze information propagation by measuring divergence after injecting noise at step  $s_t$ . We visualize CKA dissimilarity [29], where 1.0 indicates complete corruption and 0.0 indicates no effect. The results show that perturbations introduced in early diffusion steps propagate throughout the entire trajectory, fundamentally altering the final reasoning outcome. Notably, there is little recovery until the final stages, and the model does not fully recover.

Moreover, the red dotted line highlights step-wise sensitivity to disruptive noise, which gradually increases and peaks around steps 20–30. This observation aligns with our qualitative analysis. Although steps 20–30 are not the earliest stages where we first observe reasoning phenomena, by this point the model has already pruned its reasoning trajectory toward the final conclusion. Consequently, perturbations at these steps have a large impact, as they can disrupt a reasoning process that is nearly finalized. Later steps, in contrast, appear less critical for the model's reasoning capability.

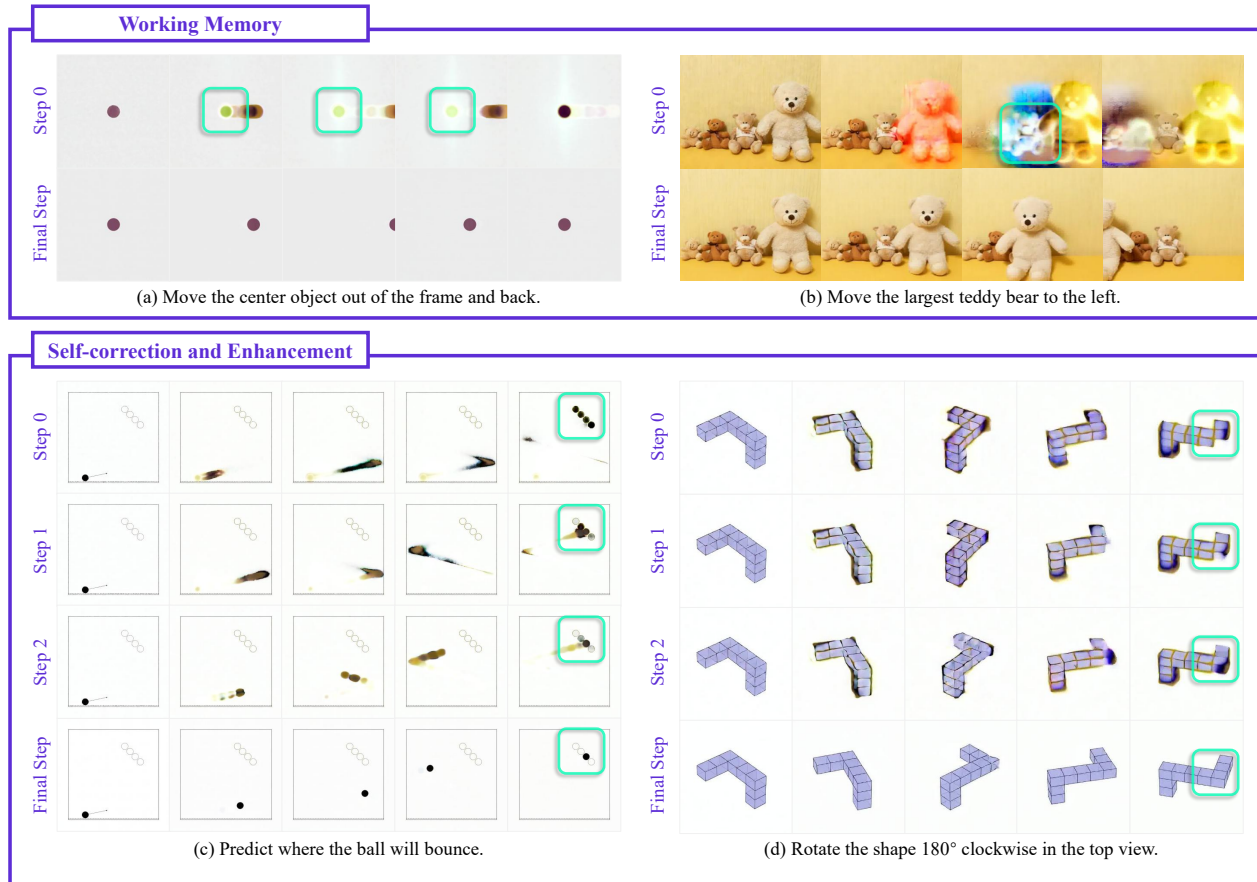


**Figure 4 Emergent reasoning behaviors: memory and self-correction.** (a) The center point is retained to guide the return motion. (b) The contour of the occluded small teddy bear is preserved, enabling the model to address object permanence. (c) The trajectory of the ball gradually extends and becomes complete. (d) The missing cube only appears in the later diffusion steps. Cyan boxes are added for illustration; they are not part of the generated video.

## 4 Emergent Reasoning Behaviors

Similar to the emergent reasoning behaviors observed in Large Language Models (LLMs), we identify three surprising properties that are critical to effective video reasoning: *working memory* (Sec. 4.1), which retains essential information throughout the reasoning process; *self-correction and enhancement* (Sec. 4.2), which enables the model to revise intermediate hypotheses or refine previously generated answers, gradually adjusting toward the optimal solution even when it is not present initially; and *perception before action* (Sec. 4.3), through which the model spontaneously develops a universal protocol within its architecture to handle diverse video reasoning tasks.

### 4.1 Working Memory

Reasoning requires the maintenance of "working memory" or a state. The demonstrations show that the diffusion process naturally establishes persistent anchors that preserve critical information across generation steps.

- *Fig. 4(a) Object Reappearance.* The model consistently preserves the object’s initial position throughout the diffusion steps, enabling the circle to return to its original location and remain consistent with the initial condition.
- *Fig. 4(b) Teddy Bear Relocation.* During the movement task, the largest teddy bear temporarily blocks the small teddy bear on the left. Despite this occlusion, the early diffusion steps retain the state of the small bear to ensure consistent generation in the whole video.

## 4.2 Self-correction and Enhancement

During the diffusion process, we observe several stochastic “aha moments,” where the model initially selects an incorrect option but later revises its reasoning after a few diffusion steps, exploring an alternative strategy. These behaviors are functionally analogous to the internal backtracking and “slow thinking” discussed in long-thinking Large Language Models (LLMs) [69]. Importantly, such transitions are not limited to correcting mistakes. The model may also refine an initially incomplete answer into a logically richer and more comprehensive one, reflecting a form of latent self-improvement rather than simple error repair.

In contrast to the “Chain-of-Frames” theory, which would require such corrections to happen sequentially across time, these reversals take place globally across all frames simultaneously within a single diffusion step. This provides strong evidence that the video generation model prioritizes global logical integrity over local, sequential frame-wise updates.

- *Fig. 4(c) Hit Target After Bounce.* Initially, the ball’s trajectory is incomplete and ambiguous. As diffusion progresses, the model gradually completes the trajectory, making it increasingly clear, and the outcome converges from four candidate points to a single correct point.
- *Fig. 4(d) 3D Shape Rotation.* At the first diffusion step, the rotated cubes are generated with incorrect quantities and arrangements. After several diffusion steps, the model gradually corrects both the number and the spatial configuration, producing a coherent and accurate final result.

## 4.3 Perception before Action

We observe a phenomenon suggesting that the diffusion trajectory first addresses the “what” and “where” of a scene before determining the “how” and “why” of its thinking progression. This process seems to suggest a “Perception before Action” transition, characterized by a shift from static grounding to dynamic reasoning. As illustrated in Fig. 5, the initial diffusion step primarily identifies the foreground entity (*e.g.*, the car or the door) specified in the prompt. At this stage, no explicit motion planning or relational transformation is observed. Instead, dynamic structure begins to emerge in later diffusion steps, where the model moves beyond static grounding and starts coordinating object motion and inter-object interactions.

# 5 Layer-wise Mechanistic Analysis

Inspired by the discovery of vision function layers in vision-language models [49], we investigate how diffusion transformers process visual information during video reasoning by analyzing the internal representations across transformer layers. Rather than focusing solely on generated outputs, we examine how hidden states evolve within the DiT backbone and how different layers contribute to semantic grounding and reasoning behaviors. Specifically, we study the model from two complementary perspectives: first, we visualize token-level activations across layers to analyze how attention and representation energy distribute over spatial-temporal regions; second, we conduct a layer-wise latent swapping experiment to causally evaluate how intermediate representations influence the final reasoning outcome. Together, these analyses provide a fine-grained view of how information is organized and progressively transformed inside the model.

## 5.1 Layer-wise Token-Level Visualization

To further investigate this transition, we analyze the internal activations of DiT blocks. During each diffusion step, we register forward hooks on the transformer blocks of the Wan2.2-I2V-A14B model. We specifically capture the hidden states from the first forward pass (the positive CFG pass) to isolate the model’s primary reasoning trajectory. The raw features are captured as a sequence of tokens with the shape  $(B, N, D)$ ,  $feat \in \mathbb{R}^{B \times N \times D}$  where  $N$  represents the total number of tokens and  $D = 5120$  is the embedding dimension. To restore the visual context, we utilize the grid dimensions  $(f, h, w)$  captured from the model’s `patch_embedding` layer to reshape the features into a 5D tensor of shape  $(B, f, h, w, D)$ . For each token at every spatial-temporal coordinate, we compute the  $L_2$  norm across the channel dimension  $D$ . This reduction produces a scalar value representing the activation intensity, or “energy”, of that specific patch. The final visualization is organized into a matrix where rows represent specific DiT layers (*e.g.*,  $L_0, L_{10}, L_{20} \dots L_{39}$ ) and columns represent sequential video frames. Each cell in the grid displays a heatmap of the calculated norms, allowing us to observe how the model’s attention shifts from coarse global structures in early layers to fine-grained logical reasoning in the deeper blocks.

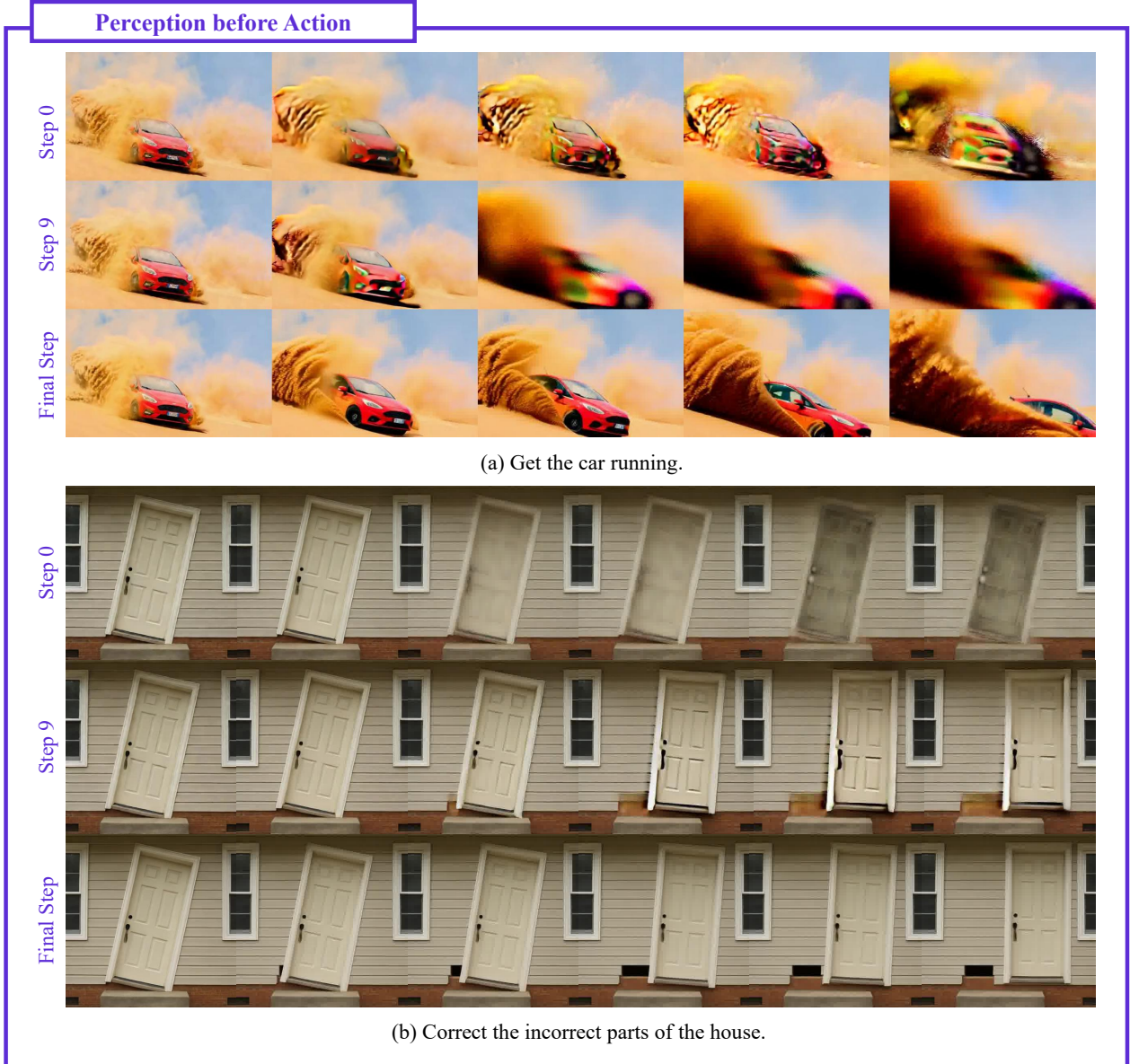


**Figure 5 Emergent reasoning behavior: understanding before reasoning.** (a) Early diffusion steps identify the car as the object of interest, while later steps introduce motion and simulate physical interactions. (b) Early steps recognize the door as the target object, and later steps manipulate it.

We observe that within a single diffusion step, the earliest layers (Layers 0–9) primarily attends to global structures and background context. As computation proceeds through the layers of the same step, attention progressively shifts toward foreground entities and those specified in the prompt. From around Layer 9 onward, activations become increasingly concentrated on semantically relevant objects, accompanied by higher channel variance in localized regions corresponding to target entities. Notably, reasoning-related features also begin to emerge at this stage, with activations correlating with object motion and interactions. This within-step progression is consistently observed across diffusion steps, indicating a recurrent hierarchy from global context to object-centric reasoning.

### 5.2 Layer-wise Latent Swapping Experiment

As illustrated in Fig. 6(b), to provide causal evidence for this transition, we conduct a layer-wise latent swapping experiment on object recognition and grounding tasks at the first diffusion step. We utilize a controlled environment featuring a blank background and two distinct sets of objects ( $O_A, O_B$ ) to perform a pair-inference task (in this case, a

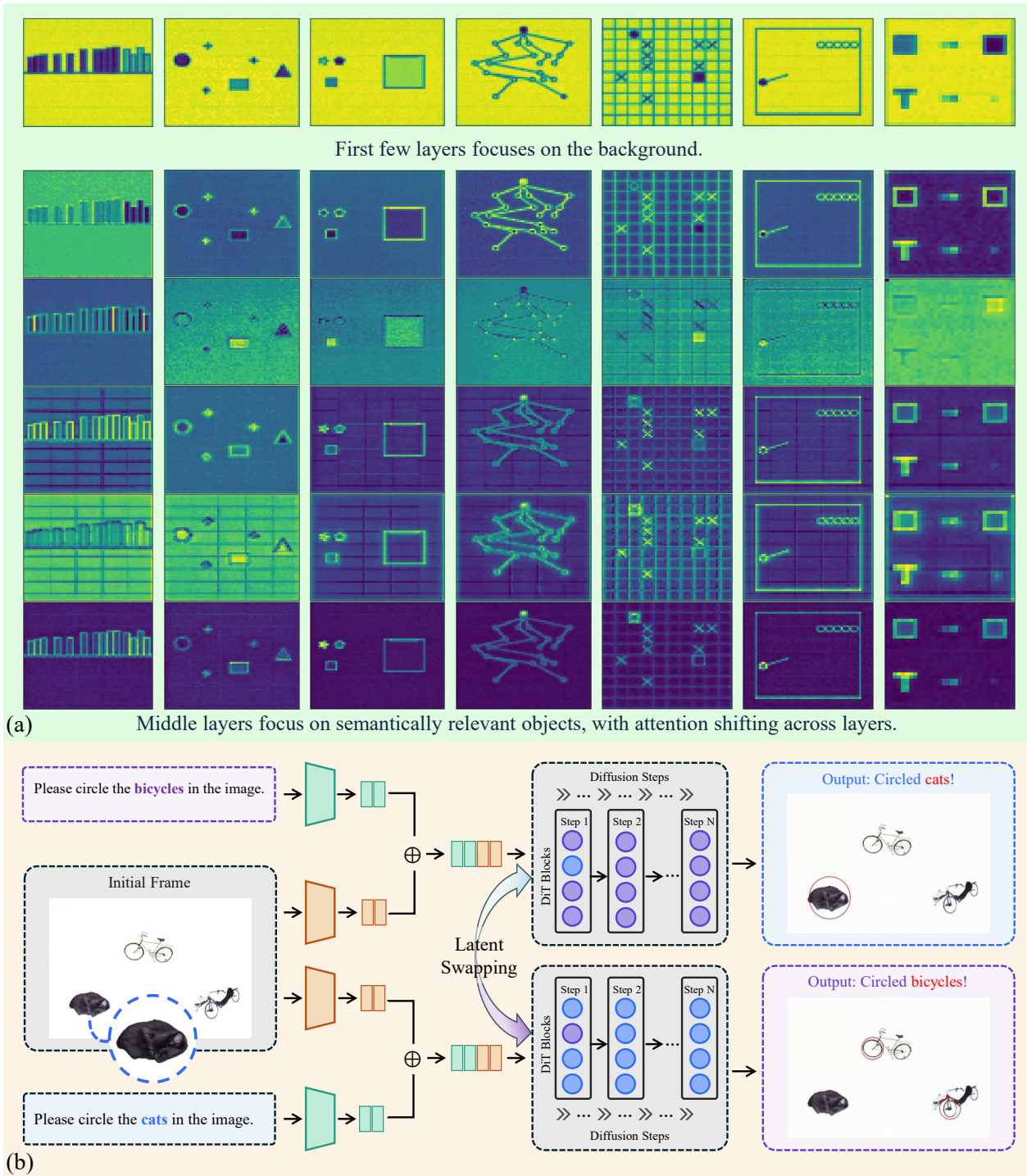


**Figure 6 Layer specialization.** (a) Layer-wise activation visualization shows that early layers of the video reasoning DiT tend to focus on background structures, whereas later layers carry out reasoning-related computations. (b) Layer-wise latent swapping reveals that certain middle layers (e.g., Layer 21 in this case) contain critical reasoning information that strongly influences the final outcome.

cat and two bicycles). Let  $U^{(l)}$  represent the latent representations (vision tokens) at layer  $l$  of the transformer backbone. To quantify the individual contribution of each layer to the final logical output, we implement a swapping operation:

$$\tilde{U}^{(k)} \leftarrow U_{alt}^{(k)}, \quad \text{subject to } U^{(l \neq k)} = U_{orig}^{(l)}$$

Models	Overall	In-Domain by Category						Out-of-Domain by Category					
		Avg.	Abst.	Know.	Perc.	Spat.	Trans.	Avg.	Abst.	Know.	Perc.	Spat.	Trans.
<b>Human</b>	0.974	0.960	0.919	0.956	1.00	0.95	1.00	0.988	1.00	1.00	0.990	1.00	0.970
<b>Open-source Video Models</b>													
CogVideoX1.5-5B-12V [70]	0.273	0.283	0.241	0.328	0.257	0.328	0.305	0.262	<u>0.281</u>	0.235	0.250	<b>0.254</b>	0.282
HunyuanVideo-12V [28]	0.273	0.280	0.207	0.357	0.293	0.280	<u>0.316</u>	0.265	<u>0.175</u>	<b>0.369</b>	0.290	<u>0.253</u>	0.250
Wan2.2-12V-A14B [57]	<b>0.371</b>	<b>0.412</b>	<b>0.430</b>	<b>0.382</b>	<b>0.415</b>	<b>0.404</b>	<b>0.419</b>	<b>0.329</b>	<b>0.405</b>	0.308	<b>0.343</b>	0.236	<u>0.307</u>
LTX-2 [17]	<u>0.313</u>	<u>0.329</u>	<u>0.316</u>	<u>0.362</u>	<u>0.326</u>	<u>0.340</u>	0.306	<u>0.297</u>	0.244	<u>0.337</u>	<u>0.317</u>	0.231	<b>0.311</b>
<b>Proprietary Video Models</b>													
Runway Gen-4 Turbo [48]	0.403	0.392	0.396	0.409	0.429	0.341	0.363	0.414	0.515	<u>0.429</u>	0.419	0.327	0.373
Sora 2 [41]	<b>0.546</b>	<b>0.569</b>	<u>0.602</u>	<u>0.477</u>	<b>0.581</b>	<b>0.572</b>	<b>0.597</b>	<b>0.523</b>	<u>0.546</u>	<b>0.472</b>	<b>0.525</b>	<b>0.462</b>	<b>0.546</b>
Kling 2.6 [30]	0.369	0.408	0.465	0.323	0.375	0.347	<u>0.519</u>	0.330	0.528	0.135	0.272	0.356	0.359
Veo 3.1 [15]	<u>0.480</u>	<u>0.531</u>	<b>0.611</b>	<b>0.503</b>	<u>0.520</u>	<u>0.444</u>	0.510	<u>0.429</u>	<b>0.577</b>	0.277	<u>0.420</u>	<u>0.441</u>	<u>0.404</u>
<b>Video Reasoning Models</b>													
VBVR-Wan2.2 [58]	<u>0.685</u>	<u>0.760</u>	<u>0.724</u>	<b>0.750</b>	<u>0.782</u>	<u>0.745</u>	<u>0.833</u>	<u>0.610</u>	<u>0.768</u>	<u>0.572</u>	<b>0.547</b>	<u>0.618</u>	<u>0.615</u>
VBVR-Wan2.2 + Training-Free Ensemble	<b>0.716</b>	<b>0.780</b>	<b>0.760</b>	<u>0.744</u>	<b>0.809</b>	<b>0.749</b>	<b>0.858</b>	<b>0.650</b>	<b>0.803</b>	<b>0.705</b>	<u>0.531</u>	<b>0.639</b>	<b>0.716</b>

**Table 1** Benchmarking results on VBVR-Bench. Overall In-Domain (ID) and Out-of-Domain (OOD) scores are reported alongside category-wise performance. Higher is better. **Bold**: best in group; underline: second best.

where  $U_{alt}^{(k)}$  contains the latent features of an alternative object configuration. The representations at all other layers remain unchanged. Strikingly, we observe that swapping the representations at layer 20 leads to a complete reversal of the inference result. That is, the model’s predicted identity of the target object flips after the substitution. This suggests that middle-to-late vision layers encode semantically decisive information that directly governs the grounding outcome.

## 6 Training-Free Ensemble

We hypothesize that while individual inference runs may exhibit stochasticity in their decisions, the reasoning manifold—the internal latent space on which the model bases its reasoning capability—often contains a shared probabilistic bias toward the correct outcome. More importantly, since the model develops multi-path reasoning during the early diffusion steps (Sec. 3.1), it is natural to exploit this property. Inspired by Model Soup [63], which merges models within the same optimization basin, we implement a multi-seed ensemble at the latent level during the early diffusion steps that are critical for the reasoning trajectory (Sec. 3.2). Specifically, we execute three independent forward passes using different initial noise seeds. During the first diffusion step ( $s = 0$ ), we extract the hidden representations  $U^{(l)}$  from the transformer backbone. Guided by our observation that reasoning-active features emerge in the mid-layers (Sec. 4.3), we perform a spatial-temporal averaging of the latents across layers 20 to 29. By aggregating representations within this specific reasoning window, we effectively perform a latent-space ensemble resembling expert voting. This operation filters out seed-specific noise and biases the model’s probability distribution toward a more stable and logically consistent latent state.

We apply this training-free ensemble approach on VBVR-Wan2.2 and evaluate it on the VBVR-Bench, a benchmark specifically designed for comprehensive assessment of video reasoning. Despite its simplicity, the ensemble method yielded a 2% absolute improvement over the strong baseline in benchmark score (Tab. 1). This performance gain confirms that the model’s internal reasoning can be "steered" toward the correct answer by simply aggregating the latent from multiple stochastic trajectories during the critical early steps of the "Perception before Action" transition, effectively exploiting the probabilistic bias inherent in the reasoning manifold.

## 7 Conclusion

In this work, we investigate the mechanisms underlying reasoning in diffusion-based video generation models. Contrary to the previously hypothesized Chain-of-Frames (CoF) mechanism, we show that reasoning primarily unfolds along the diffusion steps, which we term Chain-of-Steps (CoS), through qualitative analysis and targeted perturbation experiments. Our study further reveals several emergent reasoning behaviors, including working memory retention, self-correction during generation, and layer specialization within the DiT architecture. Motivated by these insights, we propose a simple training-free reasoning path ensemble method that achieves performance improvements over a strong baseline.

## References

- [1] Alayrac, J.B., Donahue, J., Luc, P., Miech, A., Barr, I., Hasson, Y., Lenc, K., Mensch, A., Millican, K., Reynolds, M., et al.: Flamingo: a visual language model for few-shot learning. *Advances in neural information processing systems* **35**, 23716–23736 (2022)
- [2] Bai, J., Bai, S., Yang, S., Wang, S., Tan, S., Wang, P., Lin, J., Zhou, C., Zhou, J.: Qwen-vl: A versatile vision-language model for understanding, localization, text reading, and beyond. *arXiv preprint arXiv:2308.12966* (2023)
- [3] Behrens, T.E., Muller, T.H., Whittington, J.C., Mark, S., Baram, A.B., Stachenfeld, K.L., Kurth-Nelson, Z.: What is a cognitive map? organizing knowledge for flexible behavior. *Neuron* **100**(2), 490–509 (2018)
- [4] Chen, J., Xu, Z., Pan, X., Hu, Y., Qin, C., Goldstein, T., Huang, L., Zhou, T., Xie, S., Savarese, S., et al.: Blip3-o: A family of fully open unified multimodal models-architecture, training and dataset. *arXiv preprint arXiv:2505.09568* (2025)
- [5] Chen, L.L., Ma, H., Fan, Z., Huang, Z., Sinha, A., Dai, X., Wang, J., He, Z., Yang, J., Li, C., et al.: Unit: Unified multimodal chain-of-thought test-time scaling. *arXiv preprint arXiv:2602.12279* (2026)
- [6] Chen, Z., Wu, J., Wang, W., Su, W., Chen, G., Xing, S., Zhong, M., Zhang, Q., Zhu, X., Lu, L., et al.: Internvl: Scaling up vision foundation models and aligning for generic visual-linguistic tasks. In: *Proceedings of the IEEE/CVF Conference on Computer Vision and Pattern Recognition*. pp. 24185–24198 (2024)
- [7] Chern, E., Hu, Z., Chern, S., Kou, S., Su, J., Ma, Y., Deng, Z., Liu, P.: Thinking with generated images. *arXiv preprint arXiv:2505.22525* (2025)
- [8] Deng, C., Zhu, D., Li, K., Gou, C., Li, F., Wang, Z., Zhong, S., Yu, W., Nie, X., Song, Z., et al.: Emerging properties in unified multimodal pretraining. *arXiv preprint arXiv:2505.14683* (2025)
- [9] Denton, E., Fergus, R.: Stochastic video generation with a learned prior. In: *International conference on machine learning*. pp. 1174–1183. PMLR (2018)
- [10] Duan, C., Fang, R., Wang, Y., Wang, K., Huang, L., Zeng, X., Li, H., Liu, X.: Got-r1: Unleashing reasoning capability of mllm for visual generation with reinforcement learning. *arXiv preprint arXiv:2505.17022* (2025)
- [11] Fan, W., Si, C., Song, J., Yang, Z., He, Y., Zhuo, L., Huang, Z., Dong, Z., He, J., Pan, D., et al.: Vchitect-2.0: Parallel transformer for scaling up video diffusion models. *arXiv preprint arXiv:2501.08453* (2025)
- [12] Fan, X., Qiu, Z., Wu, Z., Wang, F., Lin, Z., Ren, T., Lin, D., Gong, R., Yang, L.: Phased dmd: Few-step distribution matching distillation via score matching within subintervals. *arXiv preprint arXiv:2510.27684* (2025)
- [13] Fang, R., Duan, C., Wang, K., Huang, L., Li, H., Yan, S., Tian, H., Zeng, X., Zhao, R., Dai, J., et al.: Got: Unleashing reasoning capability of multimodal large language model for visual generation and editing. *arXiv preprint arXiv:2503.10639* (2025)
- [14] Ge, Y., Zhao, S., Zhu, J., Ge, Y., Yi, K., Song, L., Li, C., Ding, X., Shan, Y.: Seed-x: Multimodal models with unified multi-granularity comprehension and generation. *arXiv preprint arXiv:2404.14396* (2024)
- [15] Google DeepMind: Veo 3.1: Ingredients to Video. Technical Report Veo 3.1, Google DeepMind (January 2026), <https://blog.google/innovation-and-ai/technology/ai/veo-3-1-ingredients-to-video/>, released January 13, 2026
- [16] Guo, Z., Zhang, R., Tong, C., Zhao, Z., Gao, P., Li, H., Heng, P.A.: Can we generate images with cot? let’s verify and reinforce image generation step by step. *arXiv preprint arXiv:2501.13926* (2025)
- [17] HaCohen, Y., Brazowski, B., Chiprut, N., Bitterman, Y., Kvochko, A., Berkowitz, A., Shalem, D., Lifschitz, D., Moshe, D., Porat, E., Richardson, E., Shiran, G., Chachy, I., Chetboun, J., Finkelson, M., Kupchick, M., Zabari, N., Guetta, N., Kotler, N., Bibi, O., Gordon, O., Panet, P., Benita, R., Armon, S., Kulikov, V., Inger, Y., Shifan, Y., Melumian, Z., Farbman, Z.: Ltx-2: Efficient joint audio-visual foundation model (2026), <https://arxiv.org/abs/2601.03233>, submitted 6 Jan 2026
- [18] Hao, S., Sukhbaatar, S., Su, D., Li, X., Hu, Z., Weston, J., Tian, Y.: Training large language models to reason in a continuous latent space. *arXiv preprint arXiv:2412.06769* (2024)
- [19] He, X., Fan, Z., Li, H., Zhuo, F., Xu, H., Cheng, S., Weng, D., Liu, H., Ye, C., Wu, B.: Ruler-bench: Probing rule-based reasoning abilities of next-level video generation models for vision foundation intelligence. *arXiv preprint arXiv:2512.02622* (2025)
- [20] Ho, J., Jain, A., Abbeel, P.: Denoising diffusion probabilistic models. In: Larochelle, H., Ranzato, M., Hadsell, R., Balcan, M., Lin, H. (eds.) *Advances in Neural Information Processing Systems*. vol. 33, pp.

6840–6851. Curran Associates, Inc. (2020), [https://proceedings.neurips.cc/paper\\_files/paper/2020/file/4c5bcfec8584af0d967f1ab10179ca4b-Paper.pdf](https://proceedings.neurips.cc/paper_files/paper/2020/file/4c5bcfec8584af0d967f1ab10179ca4b-Paper.pdf)

- [21] Huang, J., Gu, S., Hou, L., Wu, Y., Wang, X., Yu, H., Han, J.: Large language models can self-improve. In: Proceedings of the 2023 conference on empirical methods in natural language processing. pp. 1051–1068 (2023)
- [22] Huang, Z., He, Y., Yu, J., Zhang, F., Si, C., Jiang, Y., Zhang, Y., Wu, T., Jin, Q., Chanpaisit, N., Wang, Y., Chen, X., Wang, L., Lin, D., Qiao, Y., Liu, Z.: VBench: Comprehensive benchmark suite for video generative models. In: Proceedings of the IEEE/CVF Conference on Computer Vision and Pattern Recognition (2024)
- [23] Huang, Z., Yu, N., Chen, G., Qiu, H., Debevec, P., Liu, Z.: Vchain: Chain-of-visual-thought for reasoning in video generation. arXiv preprint arXiv:2510.05094 (2025)
- [24] Huang, Z., Zhang, F., Xu, X., He, Y., Yu, J., Dong, Z., Ma, Q., Chanpaisit, N., Si, C., Jiang, Y., et al.: Vbench++: Comprehensive and versatile benchmark suite for video generative models. IEEE Transactions on Pattern Analysis and Machine Intelligence (2025)
- [25] Jiang, D., Guo, Z., Zhang, R., Zong, Z., Li, H., Zhuo, L., Yan, S., Heng, P.A., Li, H.: T2i-r1: Reinforcing image generation with collaborative semantic-level and token-level cot. arXiv preprint arXiv:2505.00703 (2025)
- [26] Kingma, D.P., Welling, M.: Auto-encoding variational bayes. arXiv preprint arXiv:1312.6114 (2013)
- [27] Koh, J.Y., Fried, D., Salakhutdinov, R.: Generating images with multimodal language models. NeurIPS (2023)
- [28] Kong, W., Tian, Q., Zhang, Z., Min, R., Dai, Z., Zhou, J., Xiong, J., Li, X., Wu, B., Zhang, J., et al.: HunyuanVideo: A systematic framework for large video generative models. arXiv preprint arXiv:2412.03603 (2024)
- [29] Kornblith, S., Norouzi, M., Lee, H., Hinton, G.: Similarity of neural network representations revisited. In: International conference on machine learning. pp. 3519–3529. PMIR (2019)
- [30] Kuaishou Technology: Kling ai launches video 2.6 model with “simultaneous audio-visual generation” capability, redefining ai video creation workflow. Press Release (December 2025), model released December 3, 2025; Press release published December 5, 2025
- [31] Li, C., Wu, W., Zhang, H., Xia, Y., Mao, S., Dong, L., Vulić, I., Wei, F.: Imagine while reasoning in space: Multimodal visualization-of-thought. arXiv preprint arXiv:2501.07542 (2025)
- [32] Li, J., Li, D., Savarese, S., Hoi, S.: Blip-2: Bootstrapping language-image pre-training with frozen image encoders and large language models. In: International conference on machine learning. pp. 19730–19742. PMLR (2023)
- [33] Li, T., Lu, Q., Zhao, L., Li, H., Zhu, X., Qiao, Y., Zhang, J., Shao, W.: Unifork: Exploring modality alignment for unified multimodal understanding and generation. arXiv preprint arXiv:2506.17202 (2025)
- [34] Liao, C., Liu, L., Wang, X., Luo, Z., Zhang, X., Zhao, W., Wu, J., Li, L., Tian, Z., Huang, W.: Mogao: An omni foundation model for interleaved multi-modal generation. arXiv preprint arXiv:2505.05472 (2025)
- [35] Lin, H., Pan, X., Huang, Z., Hou, J., Wang, J., Chen, W., He, Z., Juefei-Xu, F., Sun, J., Fan, Z., et al.: Exploring mllm-diffusion information transfer with metacanvas. arXiv preprint arXiv:2512.11464 (2025)
- [36] Lipman, Y., Chen, R.T., Ben-Hamu, H., Nickel, M., Le, M.: Flow matching for generative modeling (2023)
- [37] Liu, H., Li, C., Wu, Q., Lee, Y.J.: Visual instruction tuning (2023)
- [38] Luo, Y., Zhao, X., Lin, B., Zhu, L., Tang, L., Liu, Y., Chen, Y.C., Qian, S., Wang, X., You, Y.: V-reasonbench: Toward unified reasoning benchmark suite for video generation models. arXiv preprint arXiv:2511.16668 (2025)
- [39] Madaan, A., Tandon, N., Gupta, P., Hallinan, S., Gao, L., Wiegrefe, S., Alon, U., Dziri, N., Prabhunoye, S., Yang, Y., Welleck, S., Majumder, B.P., Gupta, S., Yazdanbakhsh, A., Clark, P.: Self-refine: Iterative refinement with self-feedback (2023)
- [40] Mattar, M.G., Lengyel, M.: Planning in the brain. Neuron **110**(6), 914–934 (2022)
- [41] OpenAI: Sora: Openai’s text-to-video model (September 2025), <https://openai.com/index/sora-is-here>, publicly released September 2025
- [42] Pan, X., Shukla, S.N., Singh, A., Zhao, Z., Mishra, S.K., Wang, J., Xu, Z., Chen, J., Li, K., Juefei-Xu, F., et al.: Transfer between modalities with metaqueries. arXiv preprint arXiv:2504.06256 (2025)
- [43] Peebles, W., Xie, S.: Scalable diffusion models with transformers. In: Proceedings of the IEEE/CVF international conference on computer vision. pp. 4195–4205 (2023)

- [44] Pfeiffer, B.E., Foster, D.J.: Hippocampal place-cell sequences depict future paths to remembered goals. *Nature* **497**(7447), 74–79 (2013)
- [45] Qin, L., Gong, J., Sun, Y., Li, T., Yang, M., Yang, X., Qu, C., Tan, Z., Li, H.: Uni-cot: Towards unified chain-of-thought reasoning across text and vision. arXiv preprint arXiv:2508.05606 (2025)
- [46] Qu, L., Zhang, H., Liu, Y., Wang, X., Jiang, Y., Gao, Y., Ye, H., Du, D.K., Yuan, Z., Wu, X.: Tokenflow: Unified image tokenizer for multimodal understanding and generation. In: Proceedings of the Computer Vision and Pattern Recognition Conference. pp. 2545–2555 (2025)
- [47] Rombach, R., Blattmann, A., Lorenz, D., Esser, P., Ommer, B.: High-resolution image synthesis with latent diffusion models. In: Proceedings of the IEEE/CVF conference on computer vision and pattern recognition. pp. 10684–10695 (2022)
- [48] Runway Research: Introducing runway gen-4: Next-generation ai models for media generation and world consistency (March 2025), <https://runwayml.com/research/introducing-runway-gen-4>, accessed January 27, 2026
- [49] Shi, C., Yu, Y., Yang, S.: Vision function layer in multimodal llms. arXiv preprint arXiv:2509.24791 (2025)
- [50] Shi, W., Han, X., Zhou, C., Liang, W., Lin, X.V., Zettlemoyer, L., Yu, L.: Lmfusion: Adapting pretrained language models for multimodal generation. arXiv preprint arXiv:2412.15188 (2024)
- [51] Shi, W., Yu, A., Fang, R., Ren, H., Wang, K., Zhou, A., Tian, C., Fu, X., Hu, Y., Lu, Z., et al.: Mathcanvas: Intrinsic visual chain-of-thought for multimodal mathematical reasoning. arXiv preprint arXiv:2510.14958 (2025)
- [52] Su, J., Lu, Y., Pan, S., Wen, B., Liu, Y.: Roformer: Enhanced transformer with rotary position embedding (2021)
- [53] Tan, Z., Yang, H., Qin, L., Gong, J., Yang, M., Li, H.: Omni-video: Democratizing unified video understanding and generation. arXiv preprint arXiv:2507.06119 (2025)
- [54] Team, C.: Chameleon: Mixed-modal early-fusion foundation models. arXiv preprint arXiv:2405.09818 (2024). <https://doi.org/10.48550/arXiv.2405.09818>, <https://github.com/facebookresearch/chameleon>
- [55] Tong, J., Mou, Y., Li, H., Li, M., Yang, Y., Zhang, M., Chen, Q., Liang, T., Hu, X., Zheng, Y., et al.: Thinking with video: Video generation as a promising multimodal reasoning paradigm. arXiv preprint arXiv:2511.04570 (2025)
- [56] Tong, S., Fan, D., Li, J., Xiong, Y., Chen, X., Sinha, K., Rabbat, M., LeCun, Y., Xie, S., Liu, Z.: Metamorph: Multimodal understanding and generation via instruction tuning. In: Proceedings of the IEEE/CVF International Conference on Computer Vision. pp. 17001–17012 (2025)
- [57] Wan, T., Wang, A., Ai, B., Wen, B., Mao, C., Xie, C.W., Chen, D., Yu, F., Zhao, H., Yang, J., et al.: Wan: Open and advanced large-scale video generative models. arXiv preprint arXiv:2503.20314 (2025)
- [58] Wang, M., Wang, R., Lin, J., Ji, R., Wiedemer, T., Gao, Q., Luo, D., Qian, Y., Huang, L., Hong, Z., Ge, J., Ma, Q., He, H., Zhou, Y., Guo, L., Mei, L., Li, J., Xing, H., Zhao, T., Yu, F., Xiao, W., Jiao, Y., Hou, J., Zhang, D., Xu, P., Zhong, B., Zhao, Z., Fang, G., Kitaoka, J., Xu, Y., Xu, H., Blacutt, K., Nguyen, T., Song, S., Sun, H., Wen, S., He, L., Wang, R., Wang, Y., Yang, M., Ma, Z., Millière, R., Shi, F., Vasconcelos, N., Khashabi, D., Yuille, A., Du, Y., Liu, Z., Lin, D., Liu, Z., Kumar, V., Li, Y., Yang, L., Cai, Z., Deng, H.: A very big video reasoning suite. arXiv preprint arXiv:2602.20159 (2026), <https://arxiv.org/abs/2602.20159>
- [59] Wang, Y., Chen, X., Ma, X., Zhou, S., Huang, Z., Wang, Y., Yang, C., He, Y., Yu, J., Yang, P., et al.: Lavie: High-quality video generation with cascaded latent diffusion models. *International Journal of Computer Vision* **133**(5), 3059–3078 (2025)
- [60] Wei, J., Tay, Y., Bommasani, R., Raffel, C., Zoph, B., Borgeaud, S., Yogatama, D., Bosma, M., Zhou, D., Metzler, D., et al.: Emergent abilities of large language models. arXiv preprint arXiv:2206.07682 (2022)
- [61] Wei, J., Wang, X., Schuurmans, D., Bosma, M., Xia, F., Chi, E., Le, Q.V., Zhou, D., et al.: Chain-of-thought prompting elicits reasoning in large language models. *Advances in neural information processing systems* **35**, 24824–24837 (2022)
- [62] Wiedemer, T., Li, Y., Vicol, P., Gu, S.S., Matarese, N., Swersky, K., Kim, B., Jaini, P., Geirhos, R.: Video models are zero-shot learners and reasoners. arXiv preprint arXiv:2509.20328 (2025)
- [63] Wortsman, M., Ilharco, G., Gadre, S.Y., Roelofs, R., Gontijo-Lopes, R., Morcos, A.S., Namkoong, H., Farhadi, A., Carmon, Y., Kornblith, S., et al.: Model soups: averaging weights of multiple fine-tuned models improves accuracy without increasing inference time. In: International conference on machine learning. pp. 23965–23998. PMLR (2022)
- [64] Wu, C., Chen, X., Wu, Z., Ma, Y., Liu, X., Pan, Z., Liu, W., Xie, Z., Yu, X., Ruan, C., et al.: Janus: Decoupling visual encoding for unified multimodal understanding and generation. arXiv preprint arXiv:2410.13848 (2024)

- [65] Wu, C., Zheng, P., Yan, R., Xiao, S., Luo, X., Wang, Y., Li, W., Jiang, X., Liu, Y., Zhou, J., et al.: Omnigen2: Exploration to advanced multimodal generation. arXiv preprint arXiv:2506.18871 (2025)
- [66] Wu, J.Z., Ren, X., Shen, T., Cao, T., He, K., Lu, Y., Gao, R., Xie, E., Lan, S., Alvarez, J.M., Gao, J., Fidler, S., Wang, Z., Ling, H.: Chronoedit: Towards temporal reasoning for image editing and world simulation. arXiv preprint arXiv:2510.04290 (2025)
- [67] Xiao, Y., Song, L., Chen, Y., Luo, Y., Chen, Y., Gan, Y., Huang, W., Li, X., Qi, X., Shan, Y.: Mindomni: Unleashing reasoning generation in vision language models with rgpo. arXiv preprint arXiv:2505.13031 (2025)
- [68] Xu, Y., Li, C., Zhou, H., Wan, X., Zhang, C., Korhonen, A., Vulić, I.: Visual planning: Let’s think only with images (2025), <https://arxiv.org/abs/2505.11409>
- [69] Yang, S., Wu, J., Chen, X., Xiao, Y., Yang, X., Wong, D.F., Wang, D.: Understanding aha moments: from external observations to internal mechanisms. arXiv preprint arXiv:2504.02956 (2025)
- [70] Yang, Z., Teng, J., Zheng, W., Ding, M., Huang, S., Xu, J., Yang, Y., Hong, W., Zhang, X., Feng, G., et al.: CogVideoX: Text-to-video diffusion models with an expert transformer. arXiv preprint arXiv:2408.06072 (2024)
- [71] Yao, S., Yu, D., Zhao, J., Shafran, I., Griffiths, T., Cao, Y., Narasimhan, K.: Tree of thoughts: Deliberate problem solving with large language models. In: Oh, A., Naumann, T., Globerson, A., Saenko, K., Hardt, M., Levine, S. (eds.) Advances in Neural Information Processing Systems. vol. 36, pp. 11809–11822. Curran Associates, Inc. (2023), [https://proceedings.neurips.cc/paper\\_files/paper/2023/file/271db9922b8d1f4dd7aaef84ed5ac703-Paper-Conference.pdf](https://proceedings.neurips.cc/paper_files/paper/2023/file/271db9922b8d1f4dd7aaef84ed5ac703-Paper-Conference.pdf)
- [72] Yao, S., Zhao, J., Yu, D., Du, N., Shafran, I., Narasimhan, K., Cao, Y.: ReAct: Synergizing reasoning and acting in language models. In: International Conference on Learning Representations (ICLR) (2023)
- [73] Yue, J., Huang, Z., Chen, Z., Wang, X., Wan, P., Liu, Z.: Simulating the visual world with artificial intelligence: A roadmap. arXiv preprint arXiv:2511.08585 (2025)
- [74] Zawalski, M., Chen, W., Pertsch, K., Mees, O., Finn, C., Levine, S.: Robotic control via embodied chain-of-thought reasoning. arXiv preprint arXiv:2407.08693 (2024)
- [75] Zeng, S., Chang, X., Xie, M., Liu, X., Bai, Y., Pan, Z., Xu, M., Wei, X.: Futuresightdrive: Thinking visually with spatio-temporal cot for autonomous driving. arXiv preprint arXiv:2505.17685 (2025)
- [76] Zhao, Q., Lu, Y., Kim, M.J., Fu, Z., Zhang, Z., Wu, Y., Li, Z., Ma, Q., Han, S., Finn, C., et al.: Cot-vla: Visual chain-of-thought reasoning for vision-language-action models. In: Proceedings of the Computer Vision and Pattern Recognition Conference. pp. 1702–1713 (2025)
- [77] Zhao, S., Zhang, Y., Cun, X., Yang, S., Niu, M., Li, X., Hu, W., Shan, Y.: Cv-vae: A compatible video vae for latent generative video models. Advances in Neural Information Processing Systems **37**, 12847–12871 (2024)
- [78] Zheng, D., Huang, Z., Liu, H., Zou, K., He, Y., Zhang, F., Zhang, Y., He, J., Zheng, W.S., Qiao, Y., Liu, Z.: VBench-2.0: Advancing video generation benchmark suite for intrinsic faithfulness. arXiv preprint arXiv:2503.21755 (2025)
- [79] Zheng, K., He, X., Wang, X.E.: Minigt-5: Interleaved vision-and-language generation via generative tokens (2023)
- [80] Zhuang, X., Xie, Y., Deng, Y., Liang, L., Ru, J., Yin, Y., Zou, Y.: Vargpt: Unified understanding and generation in a visual autoregressive multimodal large language model. arXiv preprint arXiv:2501.12327 (2025)
- [81] Zou, K., Huang, Z., Dong, Y., Tian, S., Zheng, D., Liu, H., He, J., Liu, B., Qiao, Y., Liu, Z.: Uni-mmmu: A massive multi-discipline multimodal unified benchmark. arXiv preprint arXiv:2510.13759 (2025)

# Appendix

## A More Experiments on Training-Free Ensemble

Aggregated Layers	Overall	In-Domain by Category						Out-of-Domain by Category					
		Avg.	Abst.	Know.	Perc.	Spat.	Trans.	Avg.	Abst.	Know.	Perc.	Spat.	Trans.
baseline(VBVR-Wan2.2) [58]	0.685	0.760	0.724	<b>0.750</b>	0.782	0.745	0.833	0.610	0.768	0.572	<b>0.547</b>	0.618	0.615
0-9	0.688	<u>0.774</u>	<u>0.754</u>	0.741	<u>0.808</u>	0.746	<u>0.835</u>	0.602	0.805	<u>0.635</u>	0.485	0.597	0.642
0-39	<u>0.690</u>	0.767	0.733	0.737	0.807	<u>0.747</u>	0.825	<u>0.613</u>	<b>0.830</b>	0.606	0.482	<u>0.630</u>	<u>0.657</u>
20-29(Training-Free Ensemble)	<b>0.716</b>	<b>0.780</b>	<b>0.760</b>	<u>0.744</u>	<b>0.809</b>	<b>0.749</b>	<b>0.858</b>	<b>0.650</b>	<u>0.803</u>	<b>0.705</b>	<u>0.531</u>	<b>0.639</b>	<b>0.716</b>

**Table 2** Comparison of VBVR-Bench performance across different layer windows at diffusion step  $s = 0$ . Mid-layer aggregation (20–29) achieves the best overall performance (0.716) by capturing the critical reasoning-active window. **Bold**: best in group; underline: second best.

To examine the impact of the aggregation window, we conduct an experiment over different layer ranges when performing the latent ensemble. For fair comparison, all variants perform the ensemble at the first diffusion step ( $s = 0$ ), while only the aggregated layer window is varied. As shown in Tab. 2, aggregating representations from the early layers (0–9) yields only marginal improvement over the baseline, increasing the overall score from 0.685 to 0.688, with limited gains in both in-domain and out-of-domain settings. This suggests that early-layer representations primarily encode low-level perceptual features and have not yet formed the semantic structures required for reasoning. Expanding the aggregation to all layers (0–39) produces a slightly higher overall score (0.690), but the improvement remains modest and inconsistent across categories, indicating that averaging across the entire depth introduces noise from layers that are either too early (perceptual) or too late (already specialized for generation). In contrast, aggregating mid-layer representations (layers 20–29) achieves the best performance, reaching an overall score of 0.716 and consistently improving most categories. This result aligns with our earlier analysis that the middle layers correspond to the transition stage between understanding and reasoning, where the model actively integrates semantic concepts and forms reasoning trajectories. Consequently, performing the ensemble within this reasoning-active window provides a more stable and informative latent representation, effectively filtering stochastic noise across seeds while preserving the semantic structures that guide correct reasoning.

## B The Impact of the Number of Frames

Configuration	Overall	In-Domain	Out-of-Domain
Chronoedit	0.581	0.637	0.524
5 frames	0.619	0.688	0.549
9 frames	0.632	0.716	0.549
17 frames	0.663	0.743	0.582
33 frames	0.685	0.685	0.685
65 frames	0.675	0.760	0.591
VBVR-Wan2.2	<b>0.685</b>	<b>0.760</b>	<b>0.610</b>

**Table 3** Comparison of Model Performance Across Frame Counts. Chronoedit here could be considered as a single-frame version of VBVR-Wan2.2. The original VBVR-Wan2.2 operates on  $\sim 100$  frames on average.

Although Sec. 3.1 shows that reasoning primarily occurs across diffusion steps rather than across frames, we observe that the number of frames still plays an important role. In practice, frames serve as a latent spatiotemporal workspace (or “scratchpad”) that enables the diffusion model to store essential visual information throughout the diffusion process.

In Tab. 3, following ChronoEdit [66], we conduct an experiment that repurposes the video generation model as an image editing model to simulate *single-frame* reasoning. In this setting, the 3D-factorized Rotary Position Embedding (RoPE) [52] is modified to anchor the input image at time step 0 and the output image at a predefined time step  $T$ ,

while intermediate frames are dropped after few steps. However, this configuration performs substantially worse than all *multi-frame* settings. This result suggests that maintaining multiple frames helps the model capture spatiotemporal coherence, which is critical for effective video reasoning.

We further investigate the effect of reducing the number of generated frames in VBVR-Wan2.2. The performance drop is relatively minor when the number of frames decreases from the original  $\sim 100$  to around 17. However, further reducing the frame count leads to noticeable degradation. This observation reinforces our hypothesis that although reasoning does not occur strictly in a frame-wise manner, maintaining a minimum level of temporal continuity is still necessary to accommodate key events required for correct inference.

### C Performance on 4-Step Distilled Model

We investigate how distillation affects reasoning in video generation models using a distilled 4-step Wan2.2-I2V-14B model. Distillation significantly compresses the denoising trajectory, raising the question of whether the reasoning dynamics remain observable under such a shortened inference process. To study this, we simultaneously adapt two LoRA models with scaling weights of 0.5 each: one based on VBVR-Wan2.2 that enhances reasoning capability, and the other based on a 4-step model distilled via Phased DMD [12] that improves generation speed.

We find that although the number of denoising steps is drastically reduced from 50 to 4, the steps required for reasoning cannot be compressed proportionally. In particular, the characteristic reasoning activity that typically emerges during

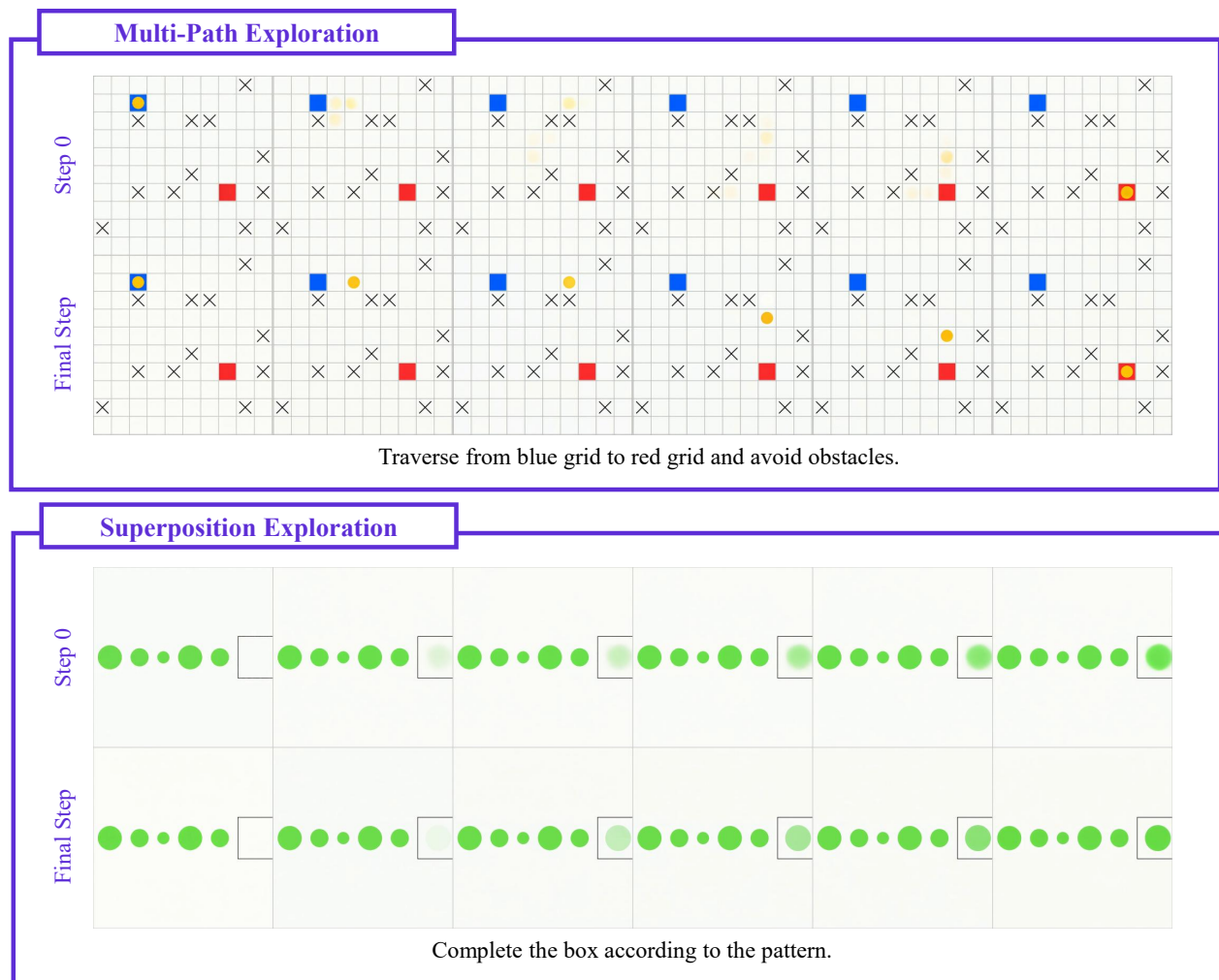
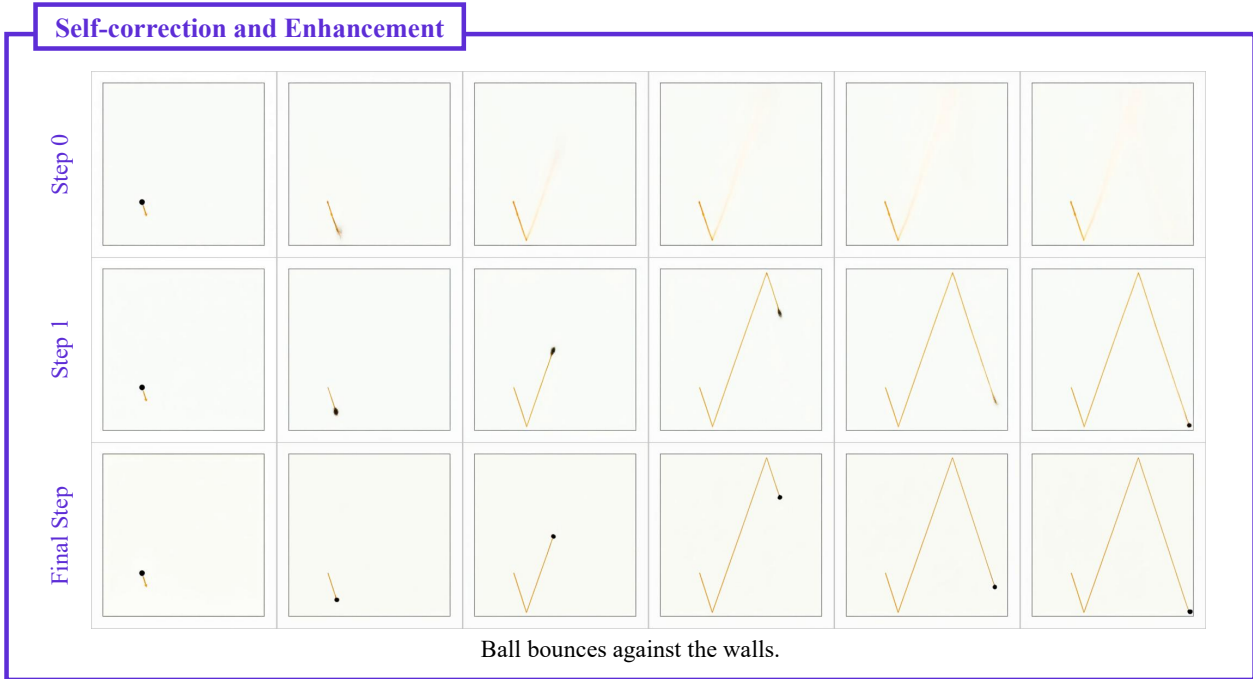
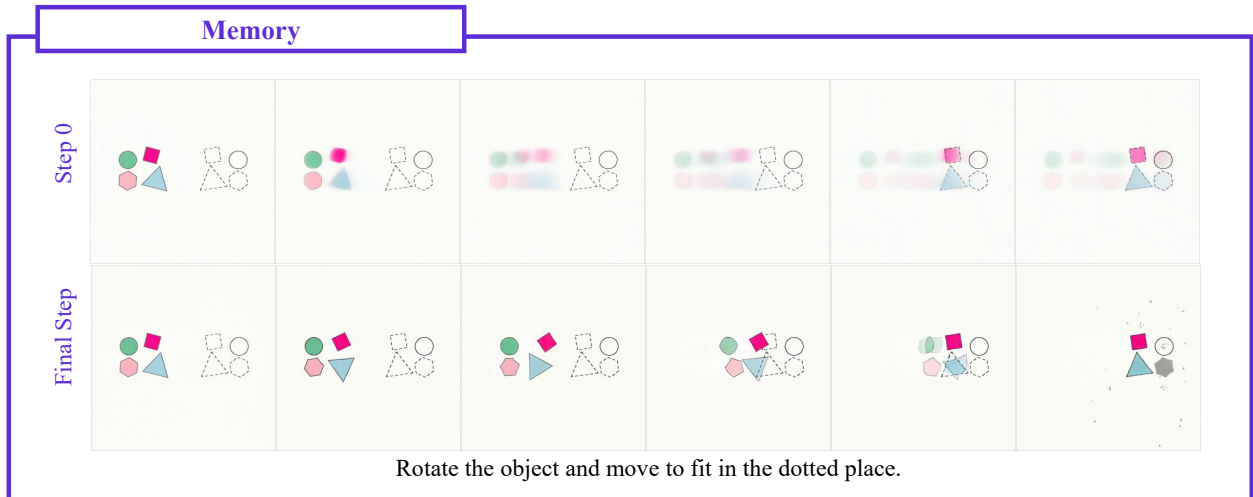


Figure 7 Qualitative visualizations of distilled model.



**Figure 7** (continued) Qualitative visualizations of distilled model.

the early diffusion steps persists even after distillation. However, we also observe that in some tasks the noise scheduler reduces the noise level too aggressively in the first step, collapsing the latent exploration phase where reasoning signals usually emerge. As a result, intermediate reasoning patterns become difficult to observe, and the overall performance on VBVR-Bench drops significantly from 0.685 to 0.605.

These results suggest that even for distilled models, preserving sufficient latent evolution during the initial diffusion step is crucial for maintaining effective reasoning capability.

## D Full Layer-wise Analysis

Sec. D.0.2 presents a comprehensive visualization of token activation energies across all 40 DiT blocks and video frames, covering all tasks reported in Sec. 5.1 and Fig. 6. Each row corresponds to a transformer block, and each column corresponds to a video frame. The heatmaps show the spatial distribution of token activation magnitudes. In Sec. 5.1,

we discuss a layer-wise transition in which early layers focus on global structures, while middle layers increasingly attend to prompt-relevant foreground objects and exhibits reasoning-related features associated with object motion and interactions. Here we discuss about two more additional findings.

#### D.0.1 High sparsity in token activations.

Across most layers, a large fraction of spatial tokens exhibit very low activation norms (dark purple regions). This indicates that only a small subset of tokens carry significant signal at any given layer. In practice, this suggests that the model performs highly sparse computation in token space, where meaningful reasoning is concentrated in localized patches corresponding to salient visual structures. Such sparsity becomes particularly pronounced in middle layers, where entire spatial regions remain near-zero while only a few tokens remain strongly active.

#### D.0.2 High concentration on token activations at middle layers.

Beginning in the intermediate layers, regular grid-like patterns become clearly visible. These patterns might align with the underlying patch tokenization structure of the transformer, potentially indicating spatial awareness. At this stage, the model may begin organizing information along patch boundaries, resulting in checkerboard- or lattice-like activation patterns.

### E More Visualization

In this section, more visualization examples are provided to further illustrate that reasoning happens across diffusion steps for video generation models. In this section, more visualization examples are provided to further illustrate that reasoning happens across diffusion steps for video generation models. These examples illustrate several recurring phenomena discussed in the main paper.

Specifically, Fig. 9 present additional cases of the *Multi-Path Exploration* phenomenon described in Sec. 3.1.1, where the model explores multiple candidate structures before converging to a coherent generation. Fig. 10 provides further examples of *Superposition-based Exploration* discussed in Sec. 3.1.2, highlighting how multiple hypotheses may coexist in intermediate representations. Fig. 11 illustrates the *Working Memory* phenomenon from Sec. 4.1, showing how the model memorises key information such as the trajectory. Finally, Figs. 12 and 13 demonstrate additional instances of *Self-correction and Enhancement* described in Sec. 4.2, where early imperfect structures are gradually refined and improved through the denoising steps.

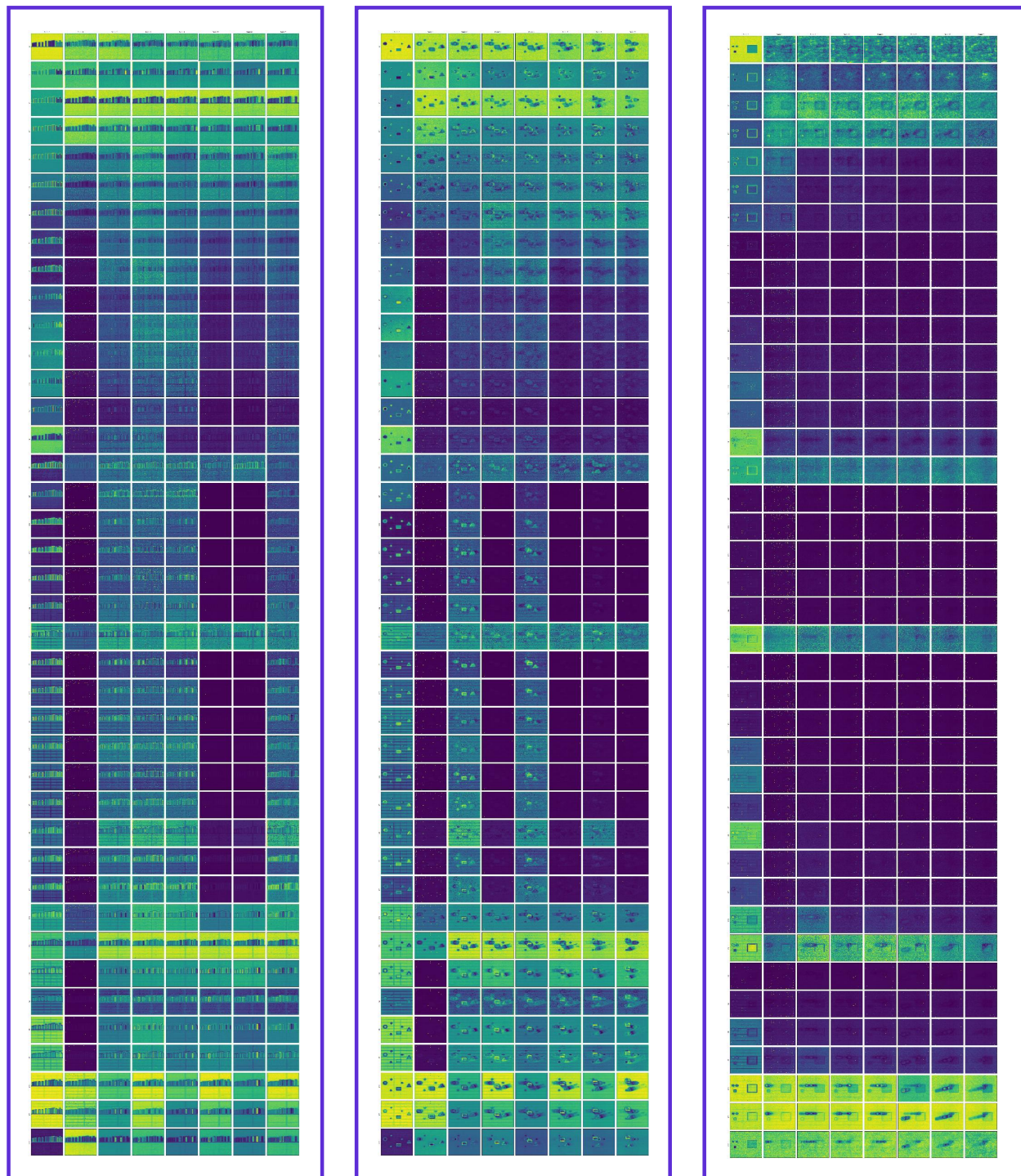


**Figure 8** Layer-wise token activation visualization across all 40 DiT blocks. Rows correspond to layers 0–39 (from top to bottom), while columns represent video frames.

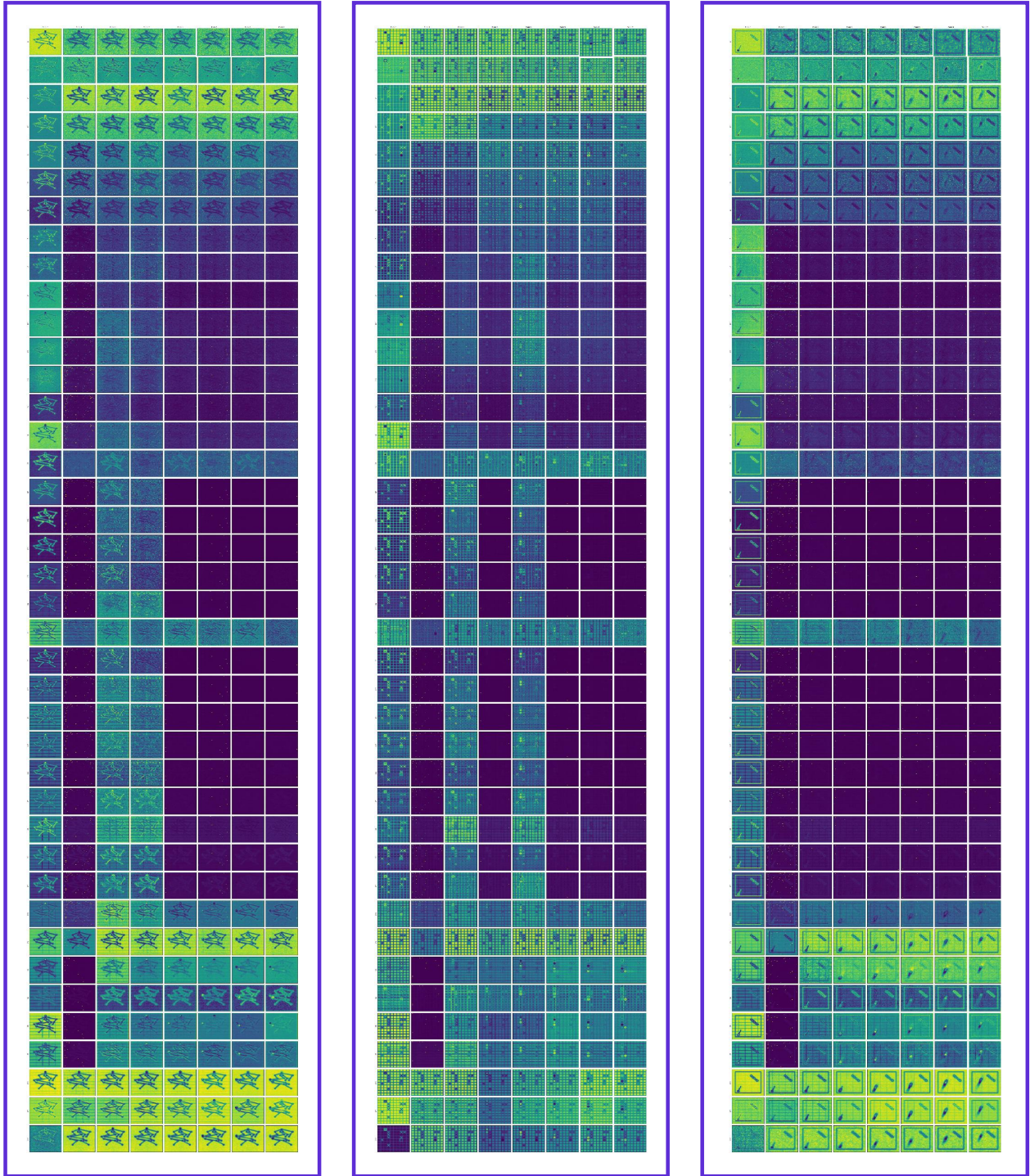


**Figure 8** (Continued) Layer-wise token activation visualization across all 40 DiT blocks. Rows correspond to layers 0–39 (from top to bottom), while columns represent video frames.

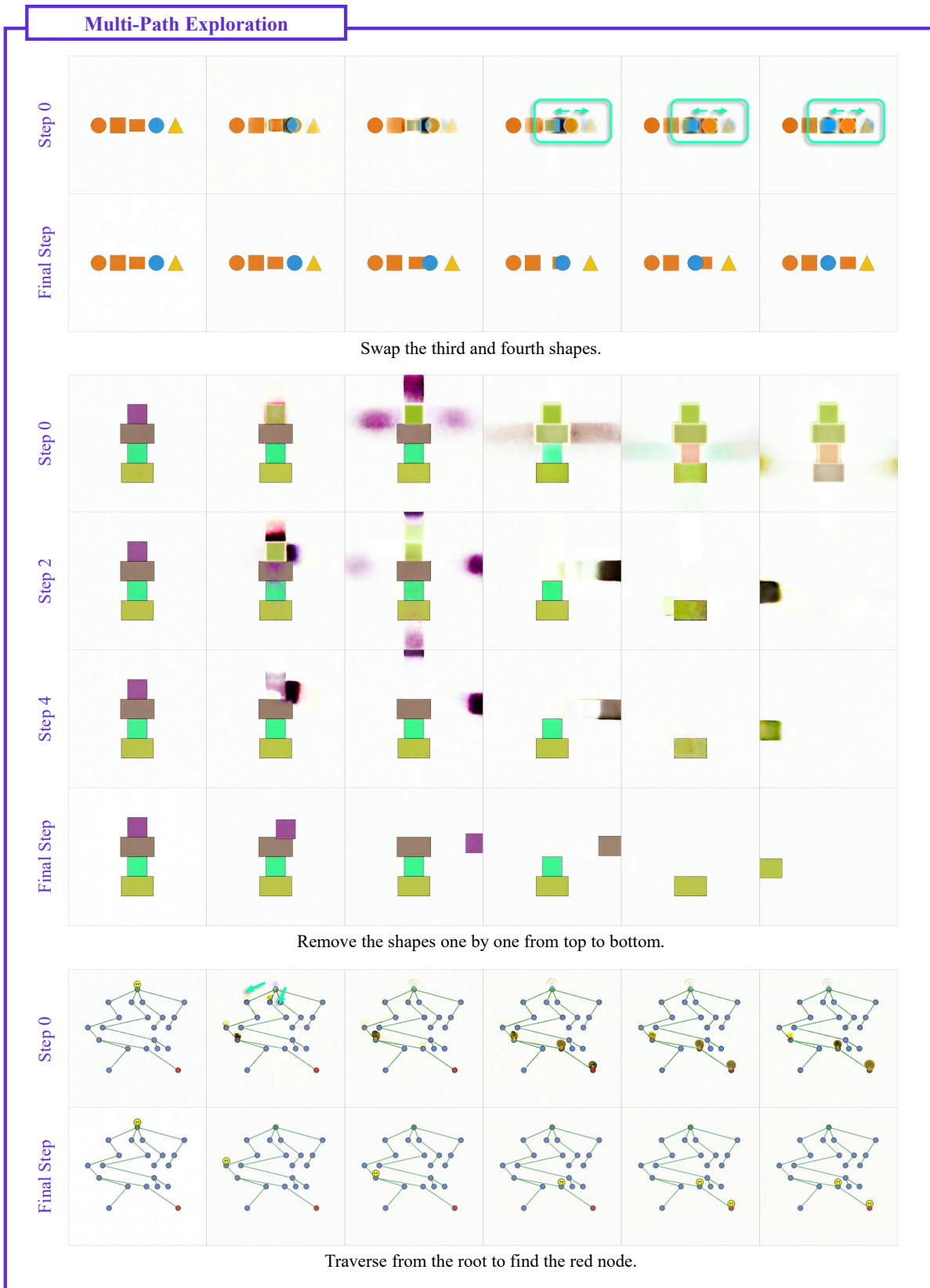
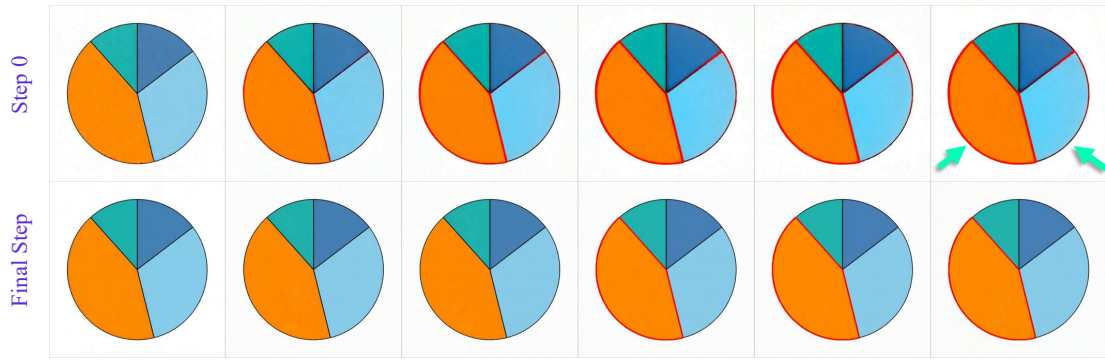
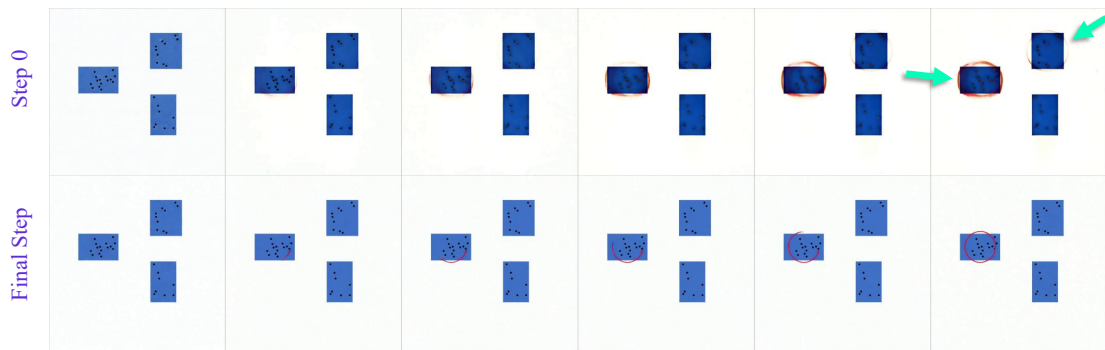


**Figure 9** More visualization of "Multi-Path Exploration" phenomenon in [Sec. 3.1.1](#).

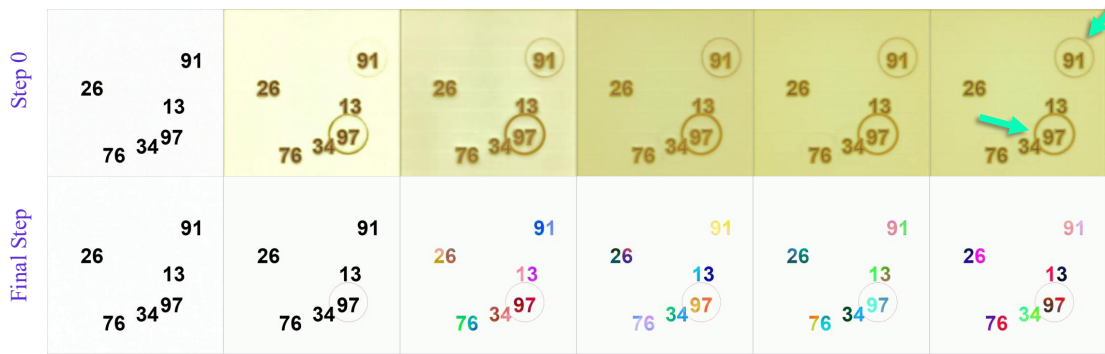
### Multi-Path Exploration



Choose the largest sector of the pie chart.



Choose the rectangle containing the maximum number of red points.



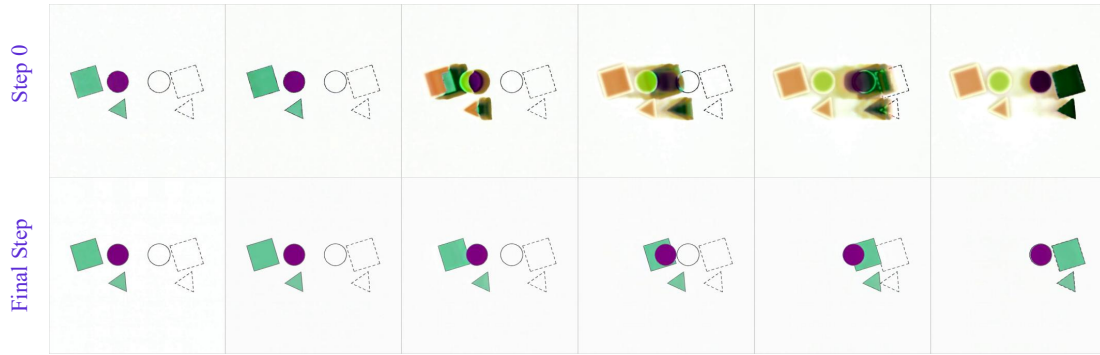
Select the largest number.

Figure 9 (Continued) More visualization of "Multi-Path Exploration" phenomenon in Sec. 3.1.1.

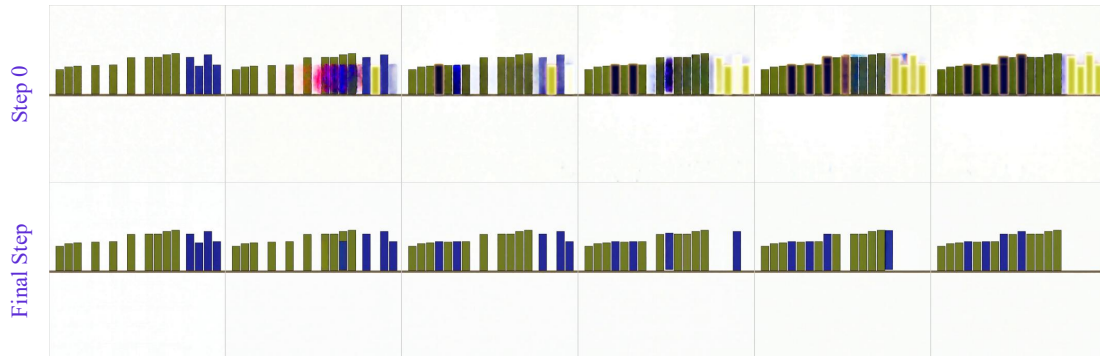


**Figure 10** More visualization of "Superposition-based Exploration" phenomenon in [Sec. 3.1.2](#).

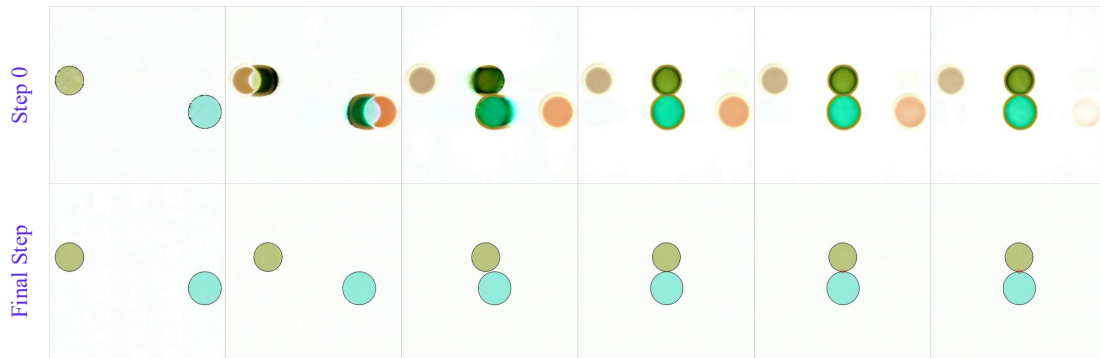
Working Memory



Move the shapes on the left into the dashed frame on the right.



Insert the blue rectangle on the left, keeping it in ascending order as much as possible.



Align the two circles centrally until they are mutually tangent.



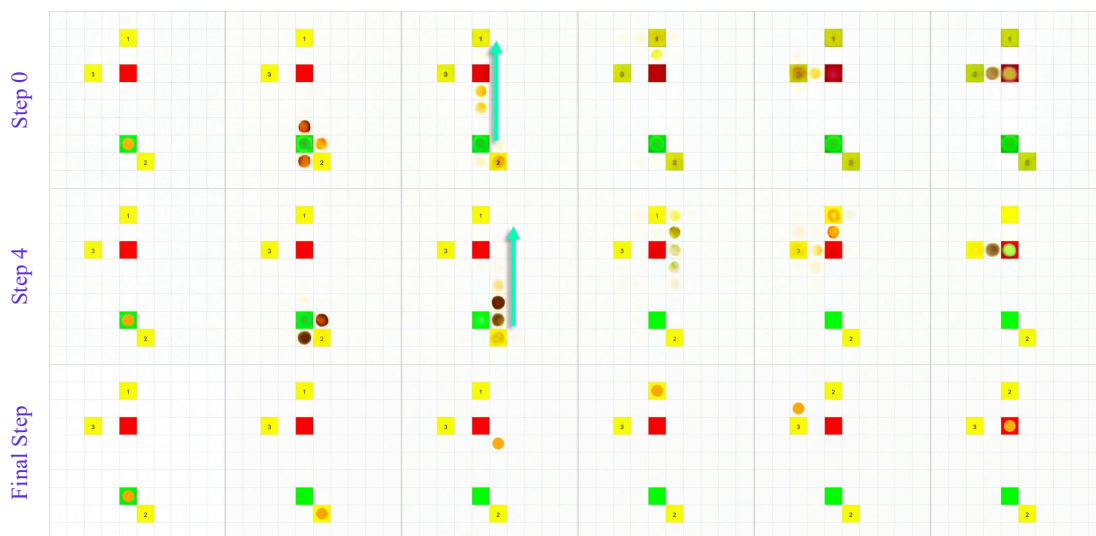
Sort the stars by size in non-decreasing order.

Figure 11 More visualization of "Memory" phenomenon in Sec. 4.1.

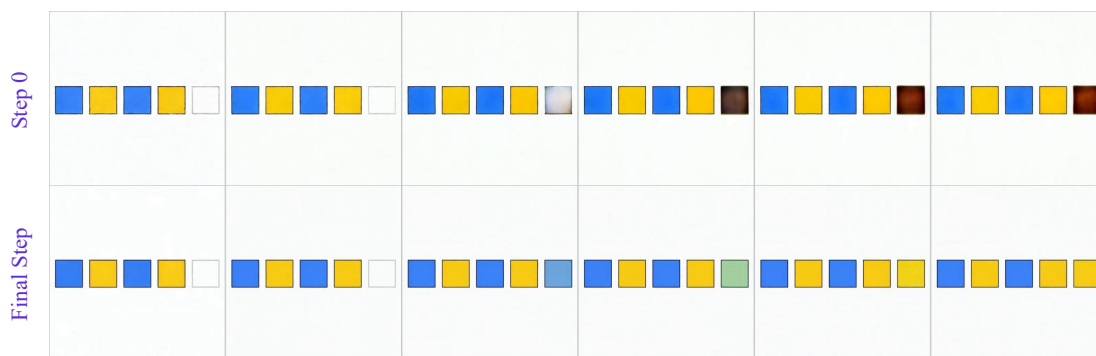
### Self-correction and Enhancement



Maximize path sum for the yellow circle from green to red via the shortest route.



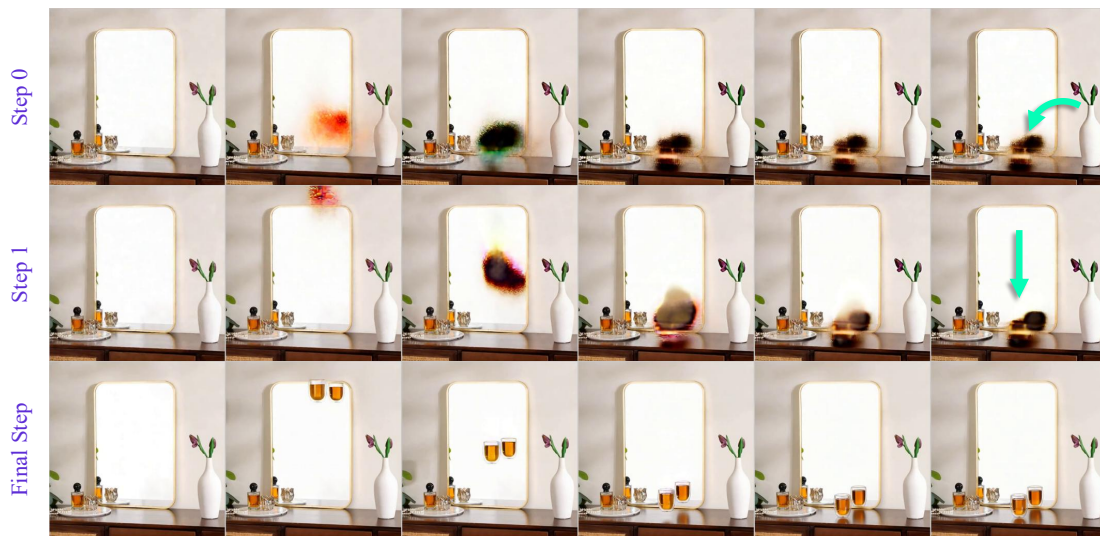
Move the yellow circle from green to red via three intermediate yellow cells.



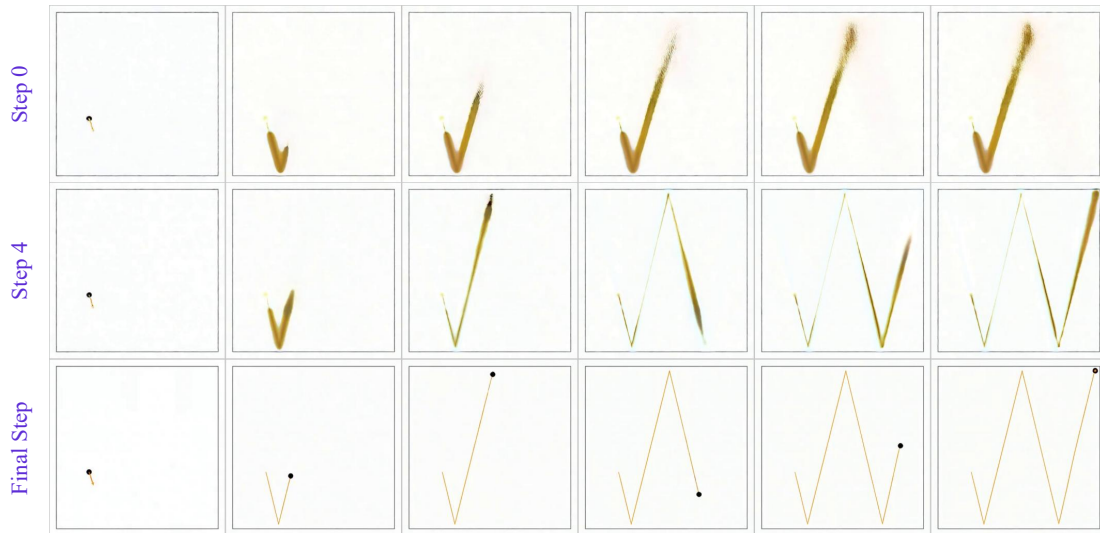
Infer the fifth square.

Figure 12 More visualization of "Self-correction and Enhancement" phenomenon in Sec. 4.2.

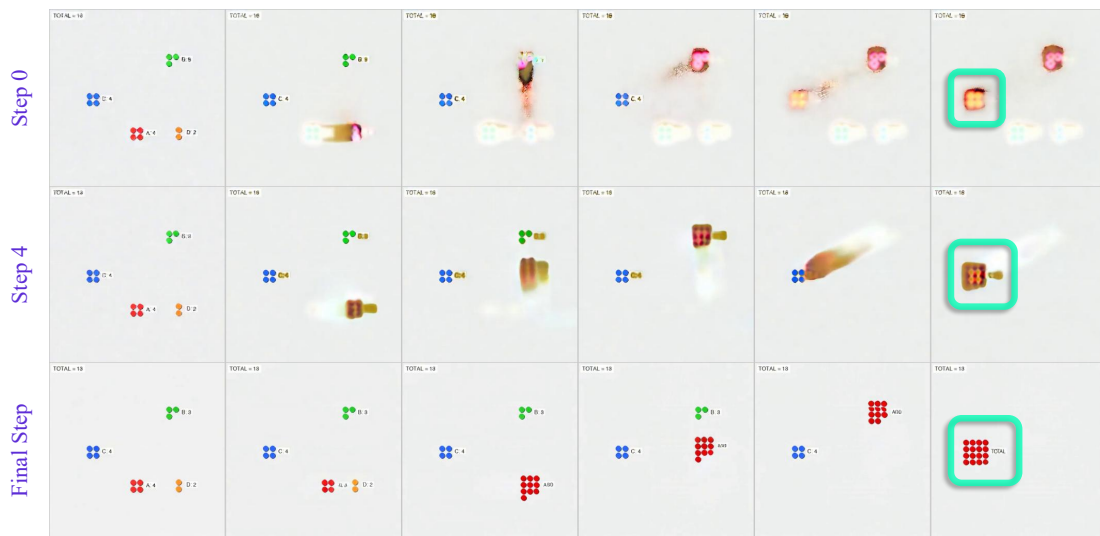
**Self-correction and Enhancement**



Place a glass of water in front of the mirror.



Predict the trajectory of the pinball.



Integrate red, orange, green, and blue groups in sequence.

**Figure 13** More visualization of "Self-correction and Enhancement" phenomenon in [Sec. 4.2](#).